POLITECNICO DI TORINO
Repository ISTITUZIONALE

Enhancing reactivity of basic oxygen furnace steel slag via aqueous carbonation in acetic acid: Influence on carbon capture, microstructure, hydration behaviour and mechanical

Original
Enhancing reactivity of basic oxygen furnace steel slag via aqueous carbonation in acetic acid: Influence on carbon capture, microstructure, hydration behaviour and mechanical properties / Ferrara, G., Humbert, P., Palmero, P.. - In: APPLIED MATERIALS TODAY. - ISSN 2352-9407. - 52:(2026), pp. 1-27. [10.1016/j.apmt.2026.103357]

Availability:
This version is available at: 11583/3013927 since: 2026-08-04T10:45:07Z

Publisher:
Elsevier

Published
DOI:10.1016/j.apmt.2026.103357

Terms of use:

This article is made available under terms and conditions as specified in the corresponding bibliographic description in the repository

Publisher copyright

(Article begins on next page)

19 November 2026

Applied Materials Today 52 (2026) 103357

Contents lists available at ScienceDirect

Applied Materials Today

journal homepage: www.elsevier.com/locate/apmt

Enhancing reactivity of basic oxygen furnace steel slag via aqueous carbonation in acetic acid: Influence on carbon capture, microstructure, hydration behaviour and mechanical properties

Giuseppe Ferrara [a,*], Pedro Humbert [b], Paola Palmero [a]

[a] Politecnico di Torino, INSTM R.U. PoliTO-LINCE, Department of Applied Science and Technology, Corso Duca Degli Abruzzi 24, Torino 10129, Italy
[b] Innovation Centre for Sustainable Construction, CRH, De Klencke 10, Amsterdam 1083 HL, Netherlands

ARTICLE INFO

Keywords:
Carbon capture and utilisation
Leaching of calcium
Mineral carbonation
Pozzolanic reactivity
Isothermal calorimetry
Bound water
Supplementary cementitious material
Compressive strength

ABSTRACT

Aqueous carbonation emerged as a valuable technique to easily induce carbon capture in Basic Oxygen Furnace (BOF) steel slag. Nevertheless, there is an increasing need for novel mineralisation processes that are aimed at enhancing the reactivity of carbonated powder to promote their employment as supplementary cementitious materials (SCM) in cement blends. This paper investigates an innovative process that integrates the leaching behaviour of an acetic acid suspension with the CO_2 mineralisation. The aim is to develop a process that enhances the pozzolanic reactivity of the carbonated particles, improves their microstructure and promotes the formation of calcium acetate contributing to the strength development. The analysis is conducted through a holistic approach, investigating: the calcium extraction capacity, the CO_2 mineralisation process, the hydration mechanisms and the mechanical performance of cement blends that include the treated powder. The results are compared with studies from the literature as well as with the performance of standardised cement. The study shows that leaching pre-treatment in acetic acid exerts a substantial influence on the hydraulic reactivity of carbonated BOF. It induces the formation of less compact calcium carbonate layers with consequent higher portlandite consumption and bound water. Moreover, it results in the formation of calcium acetate salt, which promotes the reactivity in cement blends. In fact, the compressive strength at 28 days of cementitious samples including 20% of treated powder achieves up to about 96% of plain cement. At the same time, the carbonation degree remains relevant with CO_2 uptake of 16.2% in the most reactive samples.

1. Introduction

The cement industry is currently responsible for approximately 8% of annual global anthropogenic CO_2 emissions [1]. The primary sources of these emissions are the calcination of limestone to produce clinker, accounting for approximately two-thirds of the total, and the combustion of fossil fuels, constituting around one-third. The combustion is essential for maintaining the elevated operating temperatures of the kiln, which frequently exceed 1400°C [2]. As asserted by the International Energy Agency (IEA), the approximate quantity of CO_2 generated per ton of cement is 0.60 tons [3]. Despite the relatively moderate specific emissions, a significant contribution to global CO_2 production is nevertheless made. This phenomenon can be attributed to the extensive utilisation of concrete as a construction material, with cement constituting approximately 10% of the total mass. Indeed, commencing from 1950, cement consumption has increased tenfold [4] and it is predicted to increase further by 12–23% by 2050 in comparison to 2018 levels [1]. As global infrastructure demand continues to rise, reducing the carbon footprint of cement production has become a critical challenge for achieving international climate targets. In an effort to limit the contribution of cement to global warming issue, the European Cement Association has devised a comprehensive roadmap. This roadmap meticulously delineates the potential strategies that could be employed to achieve carbon neutrality within the cement sector. These strategies encompass a range of approaches, including clinker substitution and carbon capture and utilisation (CCU) [5].

The utilisation of natural alternative binders or industrial by-products exhibiting hydraulic and/or pozzolanic behaviour in cement blends has been proposed as a strategy to reduce clinker usage. The most widely adopted supplementary cementitious materials (SCMs) are

* Corresponding author.
E-mail addresses: giuseppe.ferrara@polito.it (G. Ferrara), phumbert@crh.com (P. Humbert), paola.palmero@polito.it (P. Palmero).

https://doi.org/10.1016/j.apmt.2026.103357
Received 18 May 2026; Received in revised form 11 July 2026; Accepted 21 July 2026
Available online 31 July 2026
2352-9407/© 2026 The Author(s). Published by Elsevier Ltd. This is an open access article under the CC BY license (http://creativecommons.org/licenses/by/4.0/).

limestone, ground-granulated blast furnace slag (GGBS) and coal fly ash [6]. A number of other materials have been adopted in smaller quantities. These include silica fume, natural pozzolans, calcined clay and a range of amorphous or poorly crystalline materials containing silica, alumina and/or lime [7]. Despite the fact that the utilisation of SCM constitutes an effective strategy for reducing clinker usage, the limited supply of materials, particularly GGBS and fly ash, represents the primary constraint to further reducing the CO_2 emissions of the sector. In order to meet the increasing demand for cement, it is necessary to explore new sources of SCM. Industrial residue, such as the slag resulting from steel production, may be considered a potential SCM. This is due to the chemical composition of the residue, which contains a significant presence of free lime and calcium silicate. Nevertheless, the presence of heavy metals in steel slag imposes limitations in its applications. Furthermore, also the utilisation of slag with a reduced metal content is constrained by its diminished hydraulic reactivity, which is attributable to the slow cooling process that hinders the formation of amorphous phases [7]. In addition, a significant concern pertains to the substantial presence of CaO/MgO, which has been observed to induce volume instability issues. Consequently, further research is required to enhance the reactivity of steel slag for utilisation as SCM.

CO_2 mineralisation has emerged as a promising strategy to support net-zero emission goals. Mineralisation enables the transformation of gaseous CO_2 into stable carbonate phases, thereby ensuring permanent carbon storage. A particularly attractive route involves the aqueous carbonation of industrial byproducts in the form of powder, such as steel slags [8], cement by-pass dust [9], and other alkaline residues [10]. These materials are rich in CO_2 reactive calcium- and magnesium-related compounds that can be easily converted into carbonates with significant carbonation degree values being achieved even under mild operational conditions. This allows to permanently store CO_2, and to remove the volume instability issues related to the presence of free lime. The study from Bonfante et al. (2025) reported on the mineralisation efficiency of a large variety of industrial wastes processed via aqueous mineral carbonation [11]. The findings demonstrate that the carbonation degree at ambient temperature and pressure conditions can reach up to: 45% for basic oxygen furnace (BOF) slag, 40% for ladle furnace (LF) slag, 29% for electric arc furnace (EAF) slag, 82% for argon oxygen decarburization (AOD) slag, 66% for cement b-pass dust (CBPD) [9,12–15].

In addition to its capacity to sequester CO_2, mineralisation has been demonstrated to modify the mineral composition and the morphology of the particles. These alterations may have direct implications on the reactivity of the powders. Consequently, recent studies have investigated the use of carbonated industrial by-products as a partial replacement in cement blends [16–20]. The findings demonstrate that reactivity is associated with the composition of the material and the extent of carbonation [21]. However, the capacity of the carbonation process to enhance hydraulic or pozzolanic reactivity has been demonstrated [22].

Among the various by-products, BOF slag has attracted significant attention due to its chemical composition, which is similar to that of cementitious materials [19,20]. Indeed, in addition to ferrous phases, BOF slags primarily comprise calcium-related phases, including calcium silicates, free lime, and portlandite. However, the slow cooling often adopted to produce the waste results in the presence of calcium di-silicate, often in the crystalline form of γ-C_2S, which is characterised by low hydraulic reactivity [23]. The utilisation of mineral carbonation as a means to enhance the reactivity of BOF slag is a process that is gaining attention. Indeed, the process of extracting calcium from silicates to form carbonates has been shown to increase the availability of silica, thereby facilitating a pozzolanic effect in cementitious blends [22]. Furthermore, calcium carbonate has been observed to react with calcium aluminate from cements, forming monocarboaluminates [21,24,25]. In addition, the precipitation of carbonates on the particle generates a rough and porous structure with increased surface area. This phenomenon provides additional nucleation sites for cement hydrates [26], and it may also induce a nanofiller effect, resulting in denser structures. Li et al. (2023) [21] demonstrated that the compressive strength of cementitious pastes incorporating carbonated steel slag exhibited an increase in accordance with the carbonation degree of the powder. However, as indicated by the extant literature, even subsequent to carbonation, the BOF slag exhibits a low amorphous content, being predominantly characterised by stable crystalline phases [27]. Therefore, despite the confirmation of the capacity of carbonation to alter the microstructure and chemical composition of raw steel slag, further research in this field is necessary to enhance the reactivity to allow the use of carbonated BOF as a cement replacement [28,29].

The treatment of the steel slag in acidic suspensions is emerging as a possible strategy to improve the reactivity of the raw material. Recent studies demonstrated that the treatment of steel slag with phosphoric acid [30] or formic acid [31] may result in the modification of the microstructure of the particles, leading to an increase in surface area, and consequently, an enhancement in hydration reactivity. Nevertheless, the utilisation of strong acids gives rise to environmental concerns and safety issues. Moreover, these treatments present issues related to the recovery of the chemicals utilised. In addition to the other chemicals, the use of acetic acid was investigated [32]. The findings emphasise a beneficial effect associated with the alterations in the morphology of the particle, with an increase in superficial roughness that promotes the growth of the hydration products. In addition to being a milder acid when compared with other chemicals, the use of acetic acid has also already been widely adopted in indirect carbonation processes of steel slag. The purpose of this use is to promote the leaching of calcium before the exposure to CO_2-rich suspensions [33]. These processes have demonstrated the capacity to enhance the extent of carbonation; however, the effects on hydration are yet to be thoroughly investigated.

Recent experimental investigations showed that, during the process, acetic acid may react with the leached calcium to form calcium acetate [34]. It has been demonstrated that the presence of this compound within cement blends may have a significant impact on the hydration process. In fact, the mechanical properties of mortar samples including the steel slag treated with acetic acid were found to be enhanced in comparison to the samples that had not been treated with acid. This phenomenon can be attributed to the presence of calcium ions in calcium acetate, which, during the hydration process, fill the pores in cement paste. Moreover, a sharp increase in strength has been observed after 28 days of curing suggesting that calcium acetate strongly promotes the late-stage reactions, such as C_2S hydration and the pozzolanic reactions [35]. It has also been emphasised that high acidic concentrations reduce the pH of the cement paste, thereby hindering the hydration process. Therefore, it is imperative that the dosage of acetic acid is accurately defined in order to ensure that the beneficial effects are optimised.

The state of the art indicates that, despite the prevalence of research focusing on treatments to enhance BOF reactivity, or mineralisation processes to optimise carbon capture, there paucity of studies that address integrated processes capable of meeting both the aforementioned requirements. In order to address this gap, the present paper proposes an innovative carbonation process, with the objective of enhancing the reactivity of BOF steel slag, whilst ensuring that the relevant extent of carbonation is maintained. The process entails the utilisation of a pre-treatment in acidic conditions, subsequently followed by aqueous carbonation. Acetic acid has been selected for use in this process, as it allows for the selective leaching of calcium, thus avoiding the environmental concerns associated with the utilisation of stronger acids that are associated with the leaching of heavy metals [36]. The novelty of the study lies in the process itself. In fact, in contradistinction to the conventional indirect carbonation process, which involves the separation of solid residue from the leached suspension to yield pure calcium carbonate, this method is conducted in a single step by directly carbonating the acidic suspension.

The present study employs a systematic approach that encompasses a range of techniques of investigation, extending from microstructural levels to the strength of hardened products. The methodology has been established with the objective of demonstrating the advantageous effects associated with the process. These include the enhancement of pozzolanic reactivity of the particles due to the leaching process, which reduces the calcium content of silicates. Simultaneously, the precipitation of calcium carbonate during the carbonation process that increases the roughness of the particles, thereby affecting the hydration process. Furthermore, the formation of calcium acetate that further contributes to the enhancement of the strength of the processed powder. Concurrently, this process promotes the partial utilisation of the acid in the final product, thereby reducing issues related to recovery.

The results demonstrate that the proposed method is a valuable process to valorise the steel slag, promoting carbon capture and hydration capacity concurrently. The incorporation within cement blends of a reused material represents a significant development, paving the way for a comprehensive strategy that is aimed at reducing the environmental impact of the entire cement value chain. In this sense, the single-step process of the treatment facilitates its applicability in existing industrial systems.

The study is conducted through the investigation of the acetic acid concentration, with the objective of ascertaining the quantity that will optimise the beneficial effects. The efficiency of the process is investigated in terms of calcium leaching, carbonation and hydraulic/pozzolanic reactivity. The investigation is concluded with a focus on the mechanical performance of mortar samples, incorporating the treated powder.

2. Raw materials characterization

The Basic Oxygen Furnace steel slag (BOF) utilised in the present study originates from a steelmaking plant located in Europe. The milling of the slag was undertaken to achieve a particle size distribution analogous to that of conventional cement. The cement employed in the present study is of type CEM I 52.5 N. The chemical reagent utilised is acetic acid (purity $\geq$ 99.5%), supplied by Sigma-Aldrich.

Laser granulometry was adopted to assess particle size distribution (Malvern Mastersizer 3000E, laser diffraction particle size analyser). Fig. 1 illustrates the findings in terms of both volume density and cumulative distribution. The D_{90}, D_{50} and D_{10} characteristic values are respectively equal to 23.5 μm, 8.83 μm and 1.06 μm for BOF and 37.0 μm, 11.70 μm and 1.30 μm for cement. X-ray fluorescence analysis was adopted to assess the composition of the raw powders (Rigaku Supermini 200), which is expressed in terms of oxides wt% in Table 1. The classification of the steel slag is determined by the XRF chemical composition, and the resultant classification is then confirmed by means of a normalised CaO(MgO)-SiO_2(Na_2O, K_2O)-Al_2O_3(Fe_2O_3) phase diagram [37]. This results in the conclusion that the steel slag is of the Basic Oxygen Furnace (BOF) steel slag variety, in consistency with the information provided by the producer.

X-ray diffraction was adopted to identify the crystalline phases of the materials (Malvern Panalytical Empyrean, X-ray diffractometer). The analysis was conducted at 40 kV and 40 mA with a step size of 0.06° and 23 s per step. The 2θ range was from 5 to 70°, with a Bragg-Brentano configuration and a PIXcel detector. The XRD pattern of BOF steel slag is reported in Fig. 2a. In accordance with the XRF composition analysis, the identification of iron-related compounds was undertaken, with a notable presence of brownmillerite and wuestite. The presence of calcium di-silicate has also been observed. Intense peaks have been identified in the calcium hydroxide spectrum. The presence of portlandite can be attributed to the hydration of free lime as a result of the weathering conditions to which the BOF steel slag has been exposed when landfilled in an open field. Indeed, adding the free lime to the oxygen furnace during steel production is a common practice aimed at enhancing the slag's capacity to incorporate deleterious elements and at providing protection for the refractory walls [38]. It is evident that calcium carbonate is present in a negligible amount.

The chemical analysis indicates that the BOF steel slag exhibits a substantial abundance of Fe_2O_3. It has been demonstrated that iron-bearing phases exhibit reduced reactivity to CO_2, thereby limiting the carbonation capacity of the powder. Furthermore, the presence of heavy metals in leachate suspension may give rise to environmental concerns. In this regard, acetic acid is employed as a reagent during the leaching phase, thereby ensuring the selective leaching of calcium [36].

Thermogravimetry and differential thermal analysis were carried out by means of TG-DTA, LabSys evo machine, Setaram. The thermal treatment was carried out with a heating rate of 10 °C/min up to 1050 °C, with N_2 as carrier gas. The samples mass was equal to 50 mg. The mass losses and DTA signals in the temperature ranges 400–500 °C and 700–800 °C, respectively, confirm the presence of calcium hydroxide and calcium carbonate (see Fig. 3). It is estimated that the calcium carbonate content of the raw BOF slag, $\%CO_{2,initial}$, is equivalent to 1.1%. The mineralogical composition of cement has been identified as calcium silicates, aluminates and aluminoferrites, in conjunction to calcium sulphates (Fig. 2b). Furthermore, minor peaks indicative of calcium carbonates were identified.

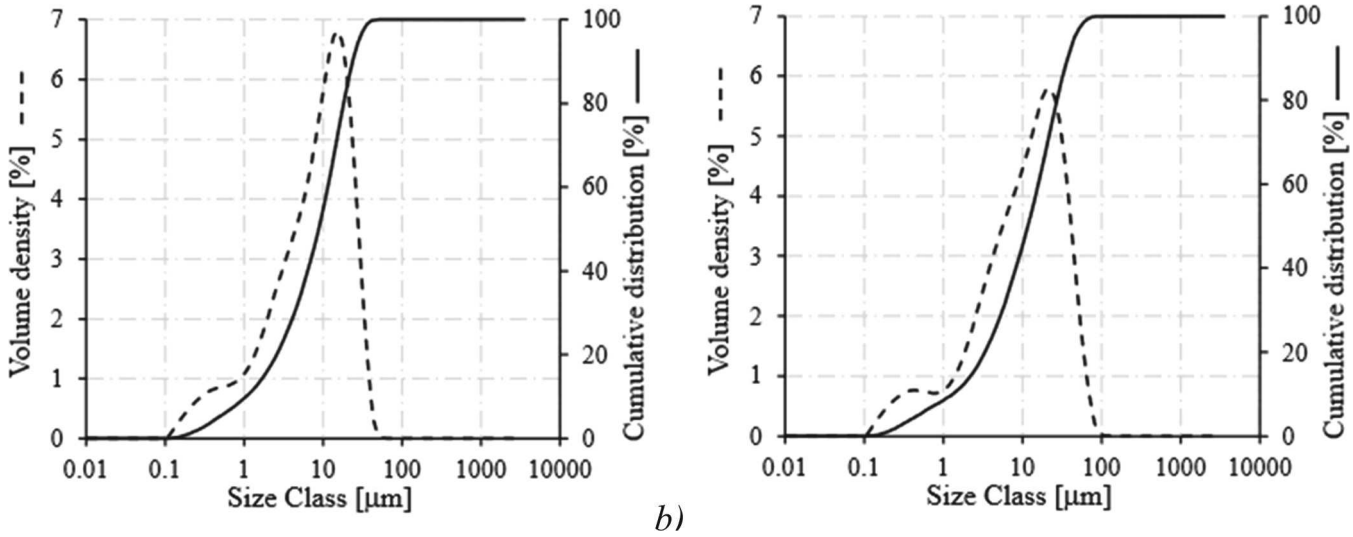


Fig. 1. Particle size distribution of: a) as received steel slag powder; b) cement powder (CEM I 52.5 N).

Table 1
Chemical composition of as received steel slag (BOF) and cement (Cem) powders (wt%).

	Na_2O	MgO	Al_2O_3	SiO_2	P_2O_5	SO_3	K_2O	CaO	TiO_2	V_2O_5	Cr_2O_3	MnO	Fe_2O_3	SrO	LOI
BOF	-	6.0	3.8	12.3	0.8	0.3		42.6	0.3	0.1	0.2	4.1	24.8	-	4.4
Cem	0.4	1.3	4.2	17.9	0.1	4.3	0.9	64.5	0.4	0.0	-	0.1	3.5	0.1	2.1

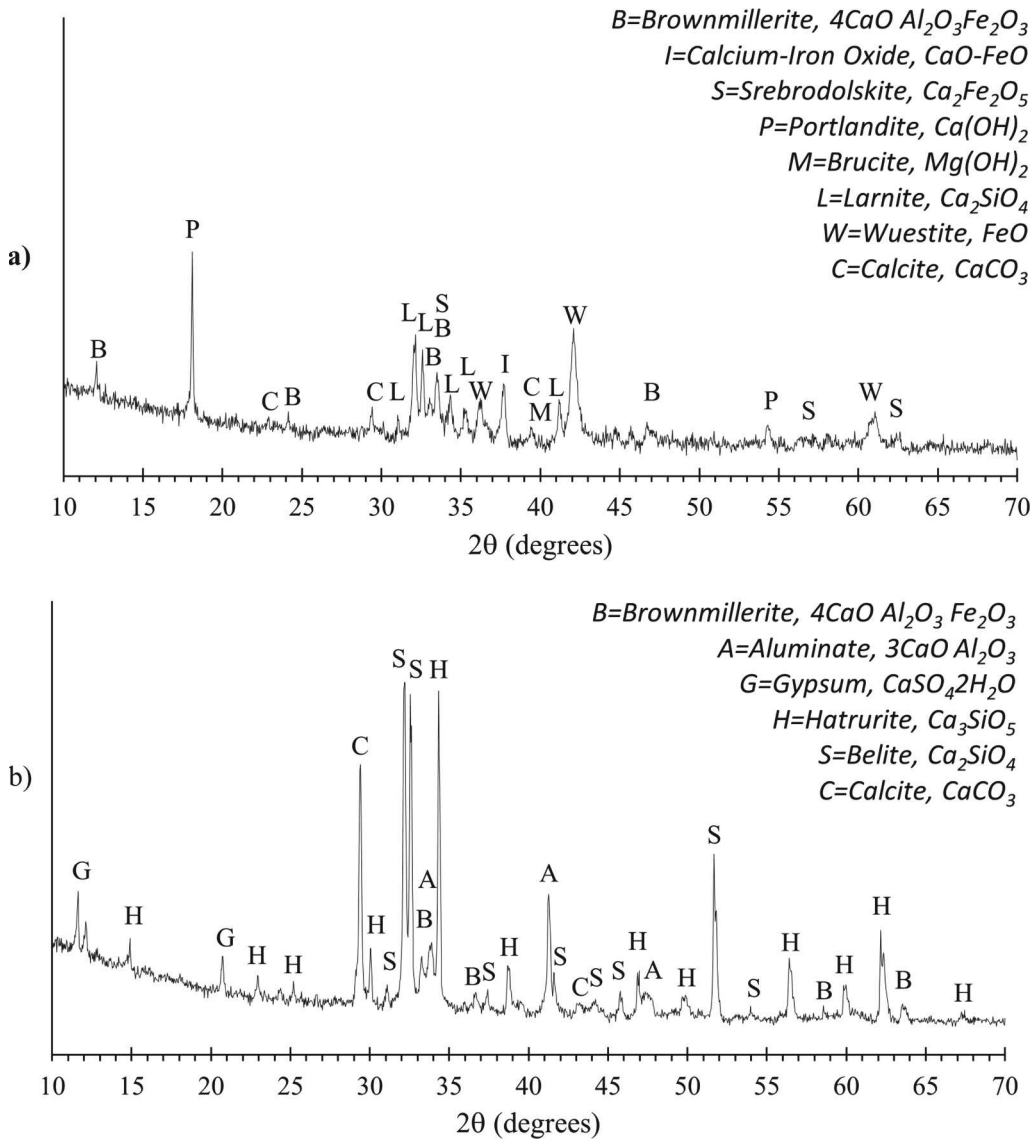


Fig. 2. XRD pattern of: a) BOF steel slag raw powder; b) cement raw powder.

3. Methods

3.1. Research plan

The research plan of the study is summarised in Fig. 4. In addition to the characterisation of raw materials, the study encompasses the various investigation steps, the respective adopted testing procedures, and the main expected outcome. Step 1 is a preliminary analysis to quantify the calcium leaching capacity of the acidic suspension. It aims at defining the adequate acid concentration and time of mixing to be adopted in the next step. Step 2 investigates the carbonation process and aims at assessing the carbonation potential of the treatment. The carbonated powders are then adopted in the Step 3 to analyse the effect of the carbonation process in terms of hydraulic and pozzolanic reactivity. Finally, the powders are adopted to partially replace cement in mortar samples for mechanical characterisation. Different curing ages are investigated in order to analyse the strength development.

3.2. Calcium extraction

Given a steel slag feedstock, the calcium extraction capacity of the acidic suspension depends on the acid concentration (herein expressed in wt%) and on the liquid-to-solid ratio (L/S) of the suspension. In fact, another important parameter is the ratio between the acid and the steel slag (g_{AA}/g_{BOF}). It emerges from the literature that g_{AA}/g_{BOF} ratios between 1 and 2.5 leads to calcium leaching rate between 70% and 100% [39–42]. This range of concentration also correspond to 2–5 vol% [39] or to 0.5–1 mol/l [42]. Based on the literature, and considering that low pH environments hinder the carbonation process, the acetic acid concentration range considered in the study reaches up to 20 wt% (that

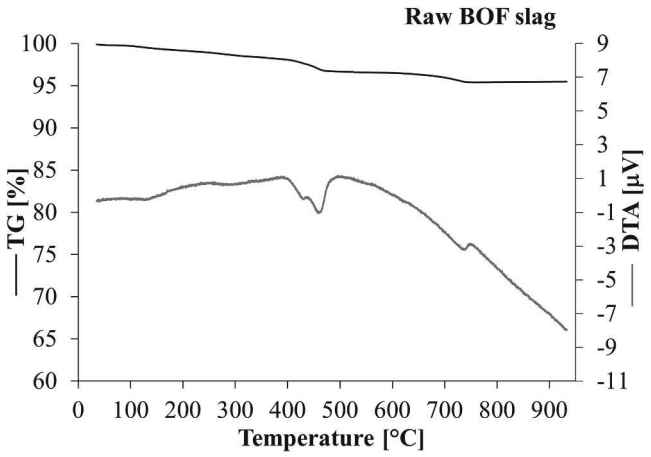


Fig. 3. TG-DTA curve of BOF steel slag raw powder.

corresponds to 1 g_{AA}/g_{BOF}).

L/S ratio is set equal to 5 to remain in the same order of previous studies from the authors (equal to 3 [9,14,43]), but at the same time to enhance the suspensibility. In fact, it was observed that significantly higher L/S values were adopted in the literature (that arrive up to 40–50 [39–42]). Time of leaching is set equal to 30 min

The various series of samples that have been adopted, in conjunction with the primary parameters considered in the leaching test, are reported in Table 2. The label of each series is characterised by "L" to indicate leaching test and "AAX%" to indicate the wt% of the acetic acid adopted.

The leaching test is carried out at ambient temperature and pressure conditions. Temperature and pressure are monitored with time interval of 5 min.

After the test, the solid fraction is extracted from the liquid suspension by means of centrifuge (10 min at 4000 rpm) and then dried for 24 h at 60 °C.

The solid residue is then analysed by means of XRD analysis. Thermogravimetry and differential thermal analysis are also carried out to complete the characterisation of the leached powder.

After each leaching test, a sample of supernatant was extracted for Inductively Coupled Plasma mass spectrometry (ICP) analysis to quantify the leached calcium expressed in ppm. The sensitivity of the instrument to detect calcium ions is in between 0.1–2 ppm. Therefore, the supernatant was diluted three times up to a factor of 1/125000, and the detected value was opportunely converted. Each ICP test provides three repetitions. The average value is considered in the analysis.

3.3. Mineralisation process

The mineralisation process is a combined leaching-carbonation procedure that comprises a pre-leaching phase in acidic conditions and a carbonation phase (Fig. 5). During the pre-leaching the suspension, with the specific acetic acid concentration, is stirred at constant rate without CO_2 injection. The operational parameters of pre-leaching phase are those defined in the previous section. After 30 min of stirring, the CO_2 pipe is immersed in the suspension to inject CO_2 gas and start the carbonation phase. The time of the carbonation phase is 60 min. The process was conducted at room temperature and pressure conditions. The CO_2 gas, with purity of 99.9% CO_2, was injected with a flow of 50 l/h. In the course of the carbonation phase temperature and pH values were monitored at regular intervals of 10 min. The entire duration of the CO_2 mineralisation process is 1.5 h. An additional measurement is provided at 5 min from the beginning of the carbonation phase. After the test, the solid fraction is extracted from the liquid suspension by centrifugation (10 min at 4000 rpm) and then drying for 24 h at 60 °C.

The carbonation test series of samples, together with the adopted proportions of materials, are reported in Table 3. The label of each series is characterised by "C" to indicate CO_2 mineralisation test and "AAX%" to indicate the wt% of the acetic acid adopted. Based on the results from leaching tests, the samples with acetic acid concentration higher than 5 wt% were not considered as characterised by low pH values, not suitable for carbonation.

XRD and TGA tests are carried out on the carbonated powder to investigate the effects of the process on the mineral composition. In addition, Field Emission Scanning Electron Microscopy (FE-SEM, Hitachi S4000) was employed to analyse the microstructure of the materials before and after the carbonation.

The efficiency of the carbonation was assessed by quantifying the

Table 2
Leaching test series.

	water	BOF	L/S	AA	time	Acetic Acid Concentration	
	[g]	[g]		[g]	[min]	[wt%]	[g_{AA}/g_{BOF}]
L_AA0%	100	20	5	-	30	-	-
L_AA1%	99	20	5	1	30	1	0.05
L_AA3%	97	20	5	3	30	3	0.15
L_AA5%	95	20	5	5	30	5	0.25
L_AA10%	90	20	5	10	30	10	0.50
L_AA20%	80	20	5	20	30	20	1.00

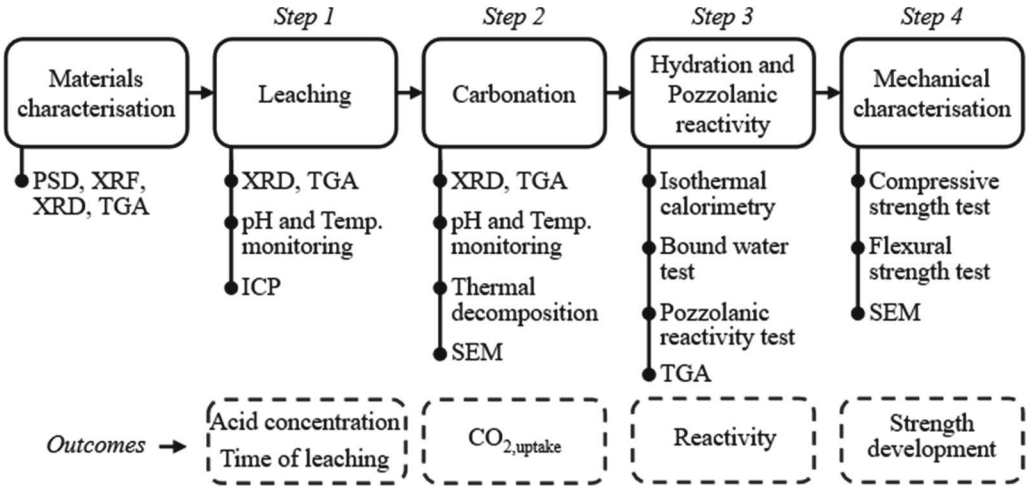


Fig. 4. Overview of the research plan: investigation steps, testing procedures and outcomes.

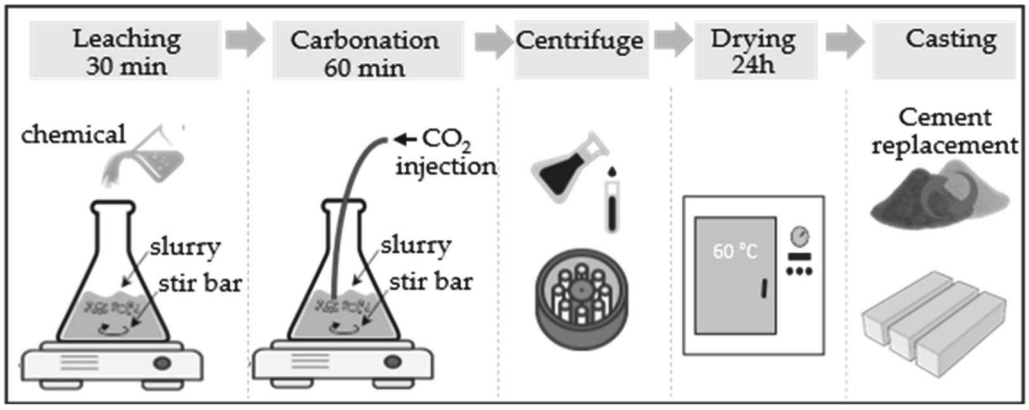


Fig. 5. Scheme of the leaching-carbonation set-up and post-treatment to extract the powder.

Table 3
Carbonation test series.

	water	BOF	L/S	AA	$time_{leach.}$	$time_{carb.}$	Acetic Acid Concentration	
	[g]	[g]		[g]	[min]	[min]	[wt%]	[g_{AA}/g_{BOF}]
C_AA0%	100	20	5	-	30	60	-	-
C_AA1%	99	20	5	1	30	60	1	0.05
C_AA3%	97	20	5	3	30	60	3	0.15
C_AA5%	95	20	5	5	30	60	5	0.25

CO_2 uptake. The CO_2 content within the carbonated powder is quantified via thermogravimetric analysis. It is assumed that the decomposition of calcium carbonate occurs between 550 °C and 850 °C [14], [44]. The CO_2 uptake, expressed as percentage of the raw material before the carbonation, is calculated by means of Eq. 1:

$$CO_{2,uptake} = \frac{\%CO_{2,content} - \%CO_{2,initial}}{1 - \%CO_{2,content}} \quad (1)$$

where $\%CO_{2,content}$ is mass loss from TG curve of the carbonated sample in the temperature range 550–850 °C, $\%CO_{2,initial}$ is the CO_2 content of the raw BOF steel slag.

Carbonated samples may include hydrated calcium acetate as a product from the reaction between the acetic acid and the calcium leached from the steel slag. The thermal decomposition of hydrated calcium acetate occurs in three steps: dehydration in the temperature range 75–187 °C; in the temperature range 334–535 °C deacetonation (DTA peak at 424 °C) and deketenation/demethanation (DTA peak at 497 °C); decarbonation in the temperature range 542–723°C [45]. The corresponding three mass-loss percentages are of 12%, 31%, and 23%, respectively. This implies that in presence of this compound, part of the CO_2 content estimated from TG-DTA derives from calcium acetate decomposition, $\Delta CO_{2,AA}$. This contribution is assessed by quantifying the calcium acetate content from the mass loss in the temperature range 334–535 °C and then considering the mass-loss percentages reported above. The mass loss was assessed via tangent method in order to ensure the calculation was not influenced by the mass loss associated with the decomposition of hydrated phases in the same range of temperature. Therefore, in case of presence of calcium acetate, the term $\%CO_{2,content}$ in Equation 1is corrected by subtracting the $\Delta CO_{2,AA}$. Similarly, considering the mass loss in the temperature range 334–535 °C corresponding to 31% in mass of the present calcium acetate, the amount of calcium acetate present in the sample, %Calc.Acet., is calculated.

The carbonated powder is adopted as cement replacement to cast mortar samples (Fig. 5). In addition to the tests described in Table 3, for each series 3 further tests were carried out in order to produce the adequate amount of powder. The carbonation efficiency of each test was assessed via thermal decomposition in muffle furnace. The experimental procedure involved a two-stage process. Initially, the sample was heated to 550°C, and the weight was recorded. Subsequently, the sample was heated to 850 °C, and the weight was recorded once more. The percentage of CO_2 content was calculated as the difference between the two recorded weights, expressed as a percentage of the initial weight at 25°C. The initial mass of the samples that were subjected to thermal decomposition in a muffle furnace was approximately 2.0 g. Three replicates were conducted for each analysed powder. The assessment of $\%CO_{2,content}$ and $\%CO_{2,uptake}$ is conducted by calculating the mean of all estimates derived from the same series of samples These estimates encompass both TG-DTA and thermal decomposition in muffle furnace analyses.

3.4. Hydration and pozzolanic reactivity tests

A series of investigative tests were conducted with the objective of determining the impact of mineralisation on the process of reactivity. This comprised calorimetry, bound water and portlandite consumption tests. The isothermal calorimetry was conducted on samples produced through the process of blending cement (CEM I 52.5 N) with the BOF slag treated with the operational parameters of the various series. The cement replacement rate and water-to-binder ratio were, respectively, set equal to 20% and 0.5 to reproduce the conditions of a possible application of the cement blend to cast mortar. The test investigates the chemical (pozzolanic or hydraulic) reactivity of the adopted powder. The objective of this study is to estimate the potential contribution of SCM to the development of strength when used with Portland cement. This will be achieved by recording the heat released during the hydration process under isothermal conditions. The experimental investigation was conducted utilising an I-Cal 8000 HPC isothermal calorimeter (Calmetrix Inc.). The instrument is equipped with eight channels, and two replicates are reproduced for each series. Each analysis is characterised by a reference sample with 100% cement content, and three other series. Therefore, two analyses were carried out in order to reproduce all the series, including reference cement, substitution with raw BOF, and substitution with carbonated BOF with acetic acid concentration varying from 0% to 5%. The details pertaining to the calorimetry test series are documented in Table 4. The test, in consistency

with bound water and portlandite consumption test, was carried out for 168 h at a temperature of 40 °C in order to accelerate the rate of reaction of slowly reactive SCMs [16,17]. Calculation of cumulative heat release started at 75 min after mixing to allow enough time for the paste and container to equilibrate at 40 ± 5 °C inside the calorimetry [16]. Initial and final setting times were determined from the derivative of the heat flow curve [17].

The R^3 method was utilised to conduct the bound water and portlandite consumption tests [46]. This implies the creation of a paste that includes portlandite, calcite and potassium solution and simulate the conditions a cementitious environment [47]. The series considered for the tests, and the respective proportions, are reported in Table 5. The results are assessed after 7 days of curing at 40 °C in sealed bags, and 24 h of drying in vacuum conditions at 40 °C (Memmert VO29). Both tests were conducted by means of TG-DTA test.

The bound water was assessed as the mass loss at a temperature of 350 °C (Eq. 2). It corresponds to the loss of the dihydroxylation and interlayer water of hydrated calcium silicates (C-S-H).

$$\%H_2O_{bound} = \frac{\Delta m_{40-350^\circ C}}{m_{dry}} \times 100 \quad (2)$$

where $\%H_2O_{bound}$ is the bound water at 7 days as percentage of the dried paste, $\Delta m_{40-350\circ C}$ is the mass loss in the temperature range 40–350 °C, m_{dry} is the initial mass of the dried sample.

The portlandite consumption test is carried out to quantify the pozzolanicity of the powder as the capacity to react with calcium hydroxide to form hydrated phases. The R^3 portlandite consumption test is carried out on a paste with known initial amount of calcium hydroxide. The quantity of portlandite consumed is determined by measuring the difference between the initial and residual calcium hydroxide levels after a period of seven days during the curing process. The residual $Ca(OH)_2$ content was evaluated through the implementation of the tangent method, a technique derived from the thermogravimetric-differential thermal analysis (TG-DTA) curve. This process provides the water loss from portlandite hydroxylation, which is then converted into consumed portlandite through stoichiometric calculation. The portlandite consumption is expressed as percentage with respect to 100 g of SCM, $\%Ca(OH)_{2,cons,SCM}$, and calculated by means of Eq. 3:

$$\%Ca(OH)_{2,cons,SCM} = \frac{\%Ca(OH)_{2,iniz} \bullet \frac{1}{\%m_{dry}} - \%Ca(OH)'_{2,final}}{\%m_{SCM} \bullet \frac{1}{\%m_{dry}}} + \%Ca(OH)_{2,raw} \quad (3)$$

where $\%Ca(OH)_{2,iniz}$ is the portlandite content of the R^3 mixture expressed as percentage of the total mass of the initial mixture; $\%Ca(OH)'_{2,final}$ is the portlandite consumption of the dried powder assessed via tangent method from TG-DTA test after 7 days of curing and 24 h of drying; $\%m_{dry}$ is the ratio between the powder after 7 days of curing and 24 h of drying and the initial mass before curing; $\%m_{SCM}$ is the ratio between the SCM mass and the total mass of the mixture; $\%Ca(OH)_{2,raw}$ is the portlandite content, if present, of the raw powder.

In the case of carbonated powder including calcium acetate, due to the decomposition of this compound in the same temperature range of calcium hydroxide, a correction is needed to properly estimate portlandite consumption. In such case the portlandite consumption is calculated by adding to the value calculated via Eq. 3 the correction value assessed via Eq. 4:

$$\%Ca(OH)_{2,AA} = \%\Delta m_{334-535,AA} \bullet \frac{\%m_{SCM}}{\%m_{dry}} \quad (4)$$

where $\%Ca(OH)_{2,AA}$ is the calcium hydroxide content associated with calcium acetate from acetic acid reaction; $\%\Delta m_{334-535,AA}$ is mass loss in the temperature range 334–535 °C calculated via TG-DTA curve of the carbonated BOF samples that include calcium acetate (samples C_AA_3% and C_AA_5%).

Bound water and portlandite consumption results of the study were compared with results assessed on conventional SCMs. These include quartz (Q), three different siliceous fly ashes (SFA_R, SFA_I, SFA_E), natural pozzolan (Po), two different calcareous fly ashes (CFA_P and CFA_S), two samples of ground granulated blast furnace slags (S1 and S8). The data are extracted from a study carried out by the technical committee RILEM TC 267-TRM that has been developing new reactivity tests for SCMs [48].

Table 5
Bound Water and Portlandite Consumption test series.

	$K^*_{solution}$	$Ca(OH)_2$	$CaCO_3$	Tested powder		Time	Temp.
	[g]			type	[g]	[h]	[°C]
RawBOF	10.8	6	1	RawBOF	2	168	40
C_AA0%	10.8	6	1	C_AA0%	2	168	40
C_AA1%	10.8	6	1	C_AA1%	2	168	40
C_AA3%	10.8	6	1	C_AA3%	2	168	40
C_AA5%	10.8	6	1	C_AA5%	2	168	40

*Ksolution : 500 ml H_2O + 2 g KOH + 10 g K_2SO_4.

3.5. Mechanical characterisation

The mechanical properties of the mortar samples were assessed in accordance with BS EN 196–1 [49]. The compressive strengths of mortars were determined by employing a hydraulic press machine (FORM+TEST Prüfsysteme MEGA 100–300–30 DM1, Riedlingen). A compressive test was conducted utilising a load cell with a capacity of 300 kN. The test involved the application of force at a rate of 1.5 kN/s, ensuring consistent and controlled conditions. Prior to conducting the compression test, prisms were cut into two halves.

Each series of samples comprised three 40×40×160 mm^3 prisms, which were cured in controlled temperature and humidity conditions of 20 °C and 100% RH, respectively. The reference series incorporated 100% CEM I 52.5 N cement as the binding agent, while all the other series utilised BOF slag with a 20% substitution in weight of cement. The complete set of samples that were given full consideration is documented in Table 6.

The fresh mixture properties were evaluated through the flow table test, which involved measuring the consistency of each batch. This was expressed in terms of the mean spreading diameter of the fresh mortar obtained after jolting the table 15 times [50]. The objective of the present study was to monitor the strength development of each series, and for this purpose, a range of curing times were considered. The duration of the period under consideration is 3 days, 7 days, 28 days and 56 days.

In light of the experimental findings, the activity index is determined as the ratio between the mean strength of the series and the mean strength of the reference CEM100%_ref series.

Table 4
Calorimetry test series.

	# samples	water	CEM I	Tested powder		Time	Temp.
		[g]	[g]	type	[g]	[h]	[°C]
CEM100%_ref	4	20	40	-	-	168	40
BOF20%_raw	2	20	32	RawBOF	8	168	40
BOF20%_C_AA0%	2	20	32	C_AA0%	8	168	40
BOF20%_C_AA1%	2	20	32	C_AA1%	8	168	40
BOF20%_C_AA3%	2	20	32	C_AA3%	8	168	40
BOF20%_C_AA5%	2	20	32	C_AA5%	8	168	40

Table 6
Mechanical test series.

		Proportions per batch					
	# batches	# samples	Sand	water	CEM I	Replacement		Curing time
			[g]	[g]	[g]	type	[g]	[days]
CEM100%_ref	4	3	1350	225	450	-	-	3, 7, 28, 56
BOF20%_raw	4	3	1350	225	360	RawBOF	90	3, 7, 28, 56
BOF20%_C_AA0%	4	3	1350	225	360	C_AA0%	90	3, 7, 28, 56
BOF20%_C_AA1%	4	3	1350	225	360	C_AA1%	90	3, 7, 28, 56
BOF20%_C_AA3%	4	3	1350	225	360	C_AA3%	90	3, 7, 28, 56
BOF20%_C_AA5%	4	3	1350	225	360	C_AA5%	90	3, 7, 28, 56

4. Results and discussion

4.1. Leaching

Leaching tests refer to the first step (depicted in Fig. 6) of the mineralisation process in which the BOF stell slag is mixed for 30 min in acid suspension. Fig. 6 shows the leached calcium expressed as function of the acetic acid concentration and assessed via ICP analysis. It emerges a linear correlation between the acetic acid concentration and the leached calcium. The absence of a plateau indicates that the adopted conditions do not allow the complete extraction of calcium. In fact, the leaching yield, expressed as the ratio between the extracted calcium and the total calcium present in the slag (from XRF analysis), attains a maximum value of 35.4%. This value is achieved in L_AA20% sample in which the amount of acetic acid equals the amount of BOF slag ($g_{AA}/g_{BOF} = 1$). Literature studies show that for acetic acid concentration of 1–1.2 g_{AA}/g_{BOF} a much higher leaching yield is obtained in the range 70–80% [39–42] (Table 7). This enhanced extraction capacity may be ascribed to the elevated liquid-to-solid ratio employed. Indeed, in the aforementioned studies, L/S values ranged between 40 and 50, while the present study adopted L/S equal to 5. As demonstrated by Mei et al. (2023), a significantly higher acetic acid concentration, approximately 7.5%, is required to achieve a higher leaching yield [40]. A comparable outcome to this study was instead reported by Klug et al. (2022) [41], irrespective of the elevated L/S ratio employed. It is important to note that the leaching yield is calculated based on the total calcium content from XRF analysis (%CaO in Table 8). However, it should be noted that not all calcium-related compounds demonstrate equivalent tendencies to leachate calcium ions. It is noteworthy that the dissolution of iron-bearing phases requires severe acidic conditions, whereas calcium silicates have been observed to release calcium ions in milder conditions. Therefore, the discrepancies of the results from the literature may also be attributed to the variability in composition of the raw material.

The pH evolution was monitored during the leaching test shown in Fig. 7a. The suspension with BOF slag (L_AA0%) is characterised by a high pH value due to the formation of calcium hydroxide, and consequent release of OH^- ions, related to the large amount of alkaline oxide, such as CaO, present in the slag. When acetic acid is present in the suspension, the initial pH is lower due to the release of H^+ ions. By increasing the acetic acid concentration, the pH of the suspension decreases. The acetic acid immediately reacts with steel slag inducing a sudden increase in the temperature (Fig. 7b). Under weak acidic conditions, as those created by acetic acid with an acid dissociation constant of 4.76, calcium extraction is promoted over Fe extraction from iron-bearing compounds of steel slag [51]. Calcium oxide and calcium silicates react with acetic acid to form calcium ions (Eq. 5, Eq. 6) [52].

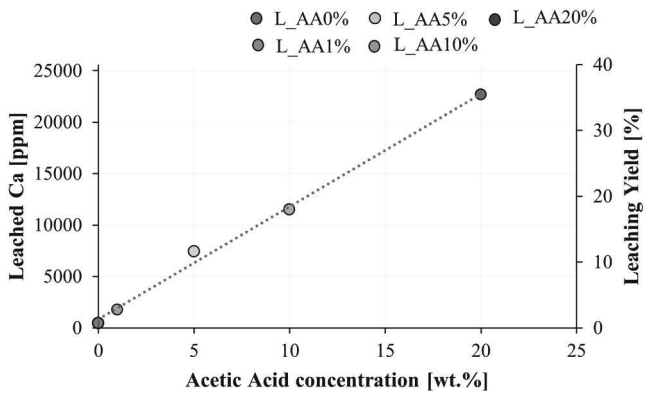


Fig. 6. Leached calcium and leaching yield as function of acetic acid concentration.

Table 7
Comparison with the literature in terms of calcium leaching yield of steel slag powders.

Study	% CaO [%]	L/S	Temp. [°C]	time min	AceticAcid/ BOF [g_{AA}/g_{BOF}]	Ca Leaching Yield [%]
This study	42.6	5	Amb.	30	1.0	35.4
Song et al. (2017)[39]	43.4	50	30	60	1.0	~70
					2.5	~100
Mei et al. (2023)[40]	46.2	125	Amb.	120	~7.5	85
Klug et al. (2022)[41]	42.2	50	Amb.	-	1.5	28.2
Liu et al. (2024)[42]	38.0	40	60	30	1.2	76.3
					2.4	~95

Table 8
$\%CO_2$ content and %calcium acetate for the different series.

	$\%CO_{2\ content,\ tot}$ [%]	$\Delta CO_{2,\ AA}$ [%]	$\%CO_{2\ content}$ [%]	RSD [%]	%Calc.Acet. [%]
RawBOF	1.1	-	1.1	-	-
C_AA0%	16.9	-	16.9	3.1	-
C_AA1%	16.9	0.1	16.8	2.8	0.6
C_AA3%	15.5	0.6	14.9	6.3	5.2
C_AA5%	15.0	1.4	13.6	3.4	11.0

$$CaO + 2CH_3COOH \rightarrow \quad Ca^{2+} + 2CH_3COO^- + 2H_2O \tag{5}$$

$$Ca_2SiO_4 + 4CH_3COOH \rightarrow \quad 2Ca^{2+} + 4CH_3COO^- + SiO_2 + 2H_2O \tag{6}$$

As the reaction progresses, acetic acid is gradually consumed, and calcium slowly dissolves. This calcium reacts with H^+ ions to form Ca^{2+} and H_2O. This results in an increase in the pH value. In the event of an excess of acetic acid, i.e. in L_AA10% and L_AA20%, the high concentration of unreacting H^+ ions reduces the pH of the suspension. It should be noted that up to a concentration of 5%, the calcium released almost compensates for the H^+ ions resulting from the dissolution of acetic acid. Consequently, when the final pH is compared with that of the reference L_AA0% sample, a moderate decrease is observed. Conversely, the final pH of the L_AA10% and L_AA20% samples was significantly lower than that of the L_AA0% reference sample. These conditions are not

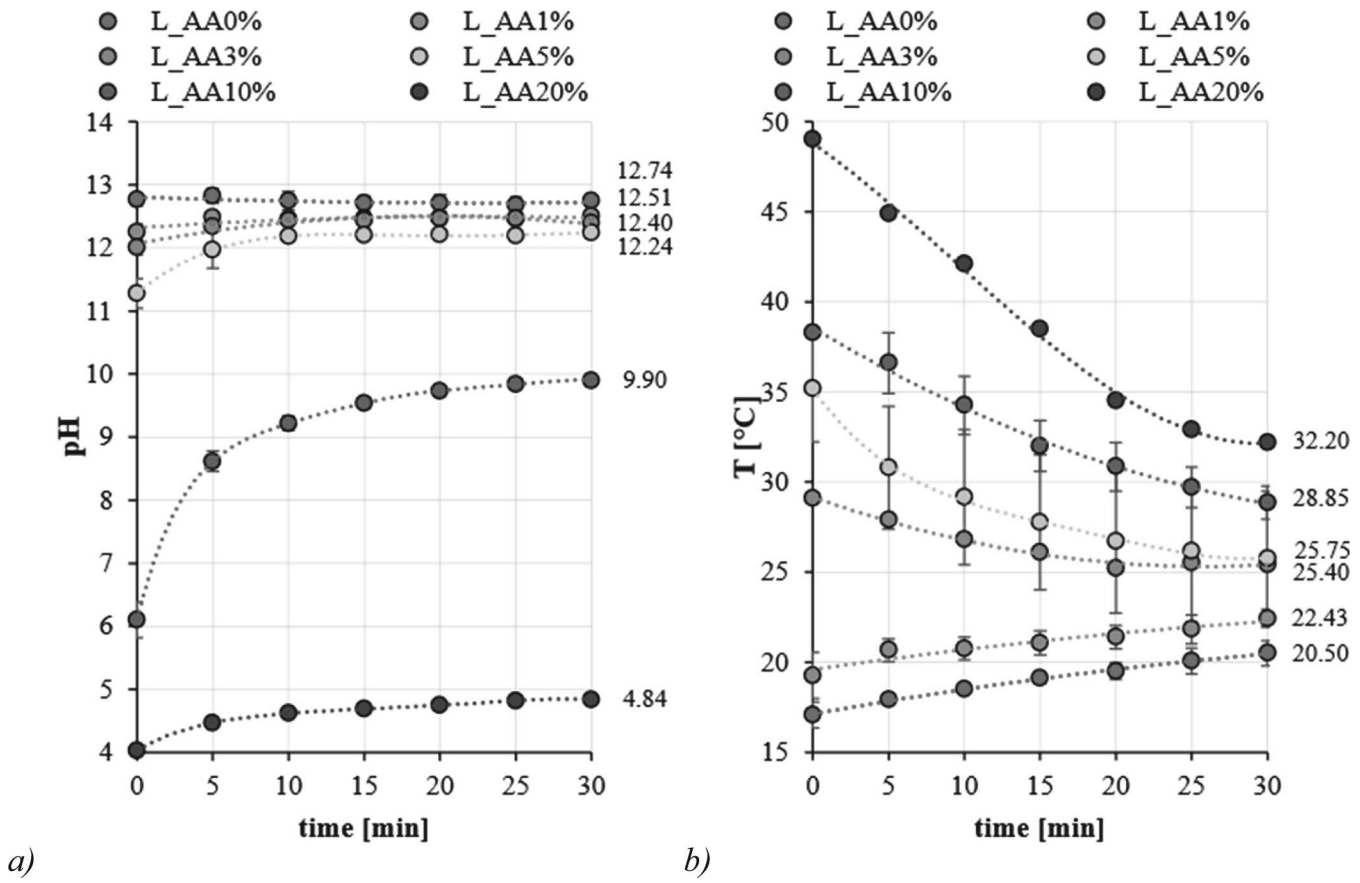


Fig. 7. a) pH and b) temperature evolution along the time of leaching tests.

favourable for carbonation reactions, since the dissolution of CO_2 into water is promoted in alkaline suspensions. Therefore, acetic acid concentrations of 10% and 20% are not considered in the subsequent carbonation stage of the study.

Fig. 7 shows that leaching time of 30 min is enough to achieve the completion of the reactions as quite stable values of pH and temperature are obtained. Fig. 8 shows the XRD pattern of the residue powder from leaching test.

The peaks of higher intensity of calcium silicate, in correspondence of 2θ angles of 32.1° and 32.6°, significantly reduce their intensity with the increase in acid content, showing the dissolution of the compound with release of calcium ions (Eq. 6). This confirms the capacity of the acetic acid to leachate calcium ions. The peaks associated with wuestite and brownmillerite do not show significant changes, confirming the poor capacity of the adopted weak acid to dissolve iron-bearing phases. The peak in correspondence of 2θ angles of 18.0°, associated with calcium hydroxide, exhibits a reduction in intensity by increasing the acetic acid concentration up to 5% and it disappears at higher concentrations. The results are corroborated by TG-DTA analysis. In fact, the presence of portlandite, emphasised by the signal II in DTA curve, is identified only in samples with acetic acid concentration lower than 5% (Fig. 9). The samples treated with high concentrations of acetic acid, L_AA10% and L_AA20%, clearly show the presence of hydrated calcium acetate. Under these conditions, the calcium ions extracted from the crystalline matrix, reacts with acetate ions to form soluble calcium acetate [42]. In fact, the centrifugation process does not completely separate the solid residue from the suspension. As consequence, part of the calcium acetate remains in the slurry, and precipitate in the form of salts during the drying process. The presence of calcium acetate is also emphasised by TG-DTA curves. In samples L_AA10% and L_AA20%, DTA signals IV and V respectively indicate the dehydration and deacetonation of hydrated calcium acetate [42]. In Fig. 9 DTA signal I indicates the presence of hydrated silicates, while DTA signal III indicates the presence of calcium carbonate. This may derive both from the carbonation of residual calcium ions in the slurry during drying process and from the decomposition of calcium acetate if present.

4.2. Carbonation

The dissolution of CO_2 gas into aqueous solution generates CO_3^{2-} ions that react with Ca^{2+} ions to form stable solid calcium carbonate. The main compounds of BOF steel slags involved in the reaction are calcium hydroxide (Eq. 7) and calcium silicates (Eq. 8). Hydrated calcium silicates may also react with CO_2 to form calcium carbonate (Eq. 9) [53]. Additional reaction products are silica gel (SiO_2) and water (H_2O).

$$Ca(OH)_2 + CO_2 \rightarrow CaCO_3 \tag{7}$$

$$2(2CaO \bullet SiO_2) + (2-x)CO_2 + yH_2O \rightarrow xCaO \bullet SiO_2 \bullet yH_2O + (2-x)CaCO_3 \tag{8}$$

$$CaO \bullet SiO_2 \bullet xH_2O + CO_2 \rightarrow \quad CaCO_3 + SiO_2 \bullet xH_2O \tag{9}$$

The XRD pattern of carbonated steel slag C_AA0% shows a clear reduction in calcium silicate peaks, and the complete absence of calcium hydroxide peaks, compared to raw BOF slag (Fig. 10). A significant increase in calcium carbonate peaks is observed. This indicates the complete carbonation of portlandite and partial consumption of calcium silicates. Conversely, iron-related phases are not significantly involved in the carbonation process as their presence remains quite unchanged in XRD pattern, confirming their low reactivity.

The XRD pattern associated with the samples carbonated in acidic conditions does not significantly differ from carbonated sample

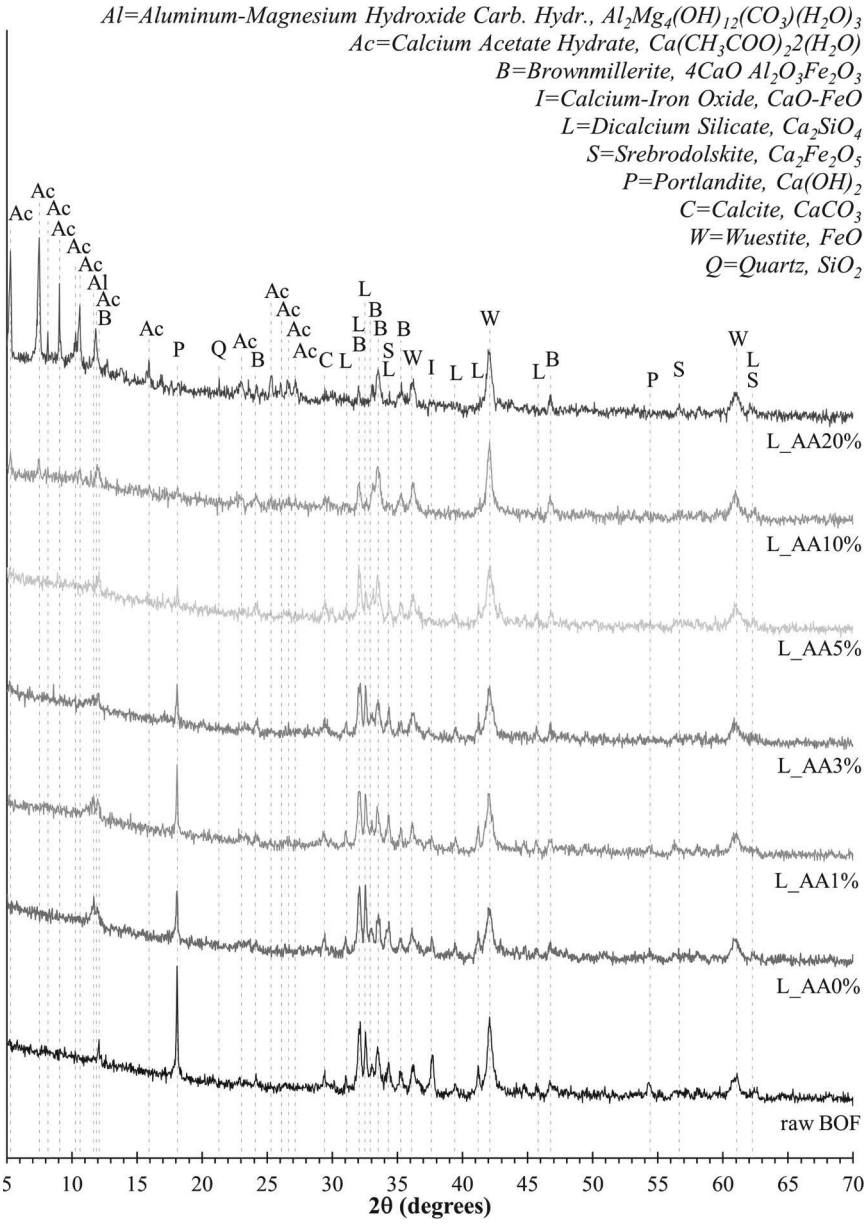


Fig. 8. XRD pattern of raw BOF and samples of leaching tests.

C_AA0%. A fair reduction in the intensity of the main peak of calcium carbonate, at 2θ of 29.5°, is observed in C_AA3% sample. This reduction becomes more pronounced in C_AA5% sample. A minor presence of calcium acetate is also observed in C_AA3% and C_AA5% samples.

The pH and temperature values were monitored during the carbonation test (Fig. 11, Fig. 12). The first 30 min concerns the mixing of the slurry in acidic conditions, the next 60 min represents the carbonation phase. In consistency with the results from the leaching study, the higher the acid concentration, the lower is the pH at the beginning of the carbonation phase. When the CO_2 is injected in the suspension (at time of 30 min) the carbonation reactions immediately take place. This generates a sudden decrease in the pH and an increase in temperature due to the exothermic carbonation reactions. These variations in pH and temperature appear to accelerate with the increase in acetic acid concentration. This is due to the higher concentration of calcium ions after the leaching process (Fig. 6) that are immediately available for carbonation. In all the series at around 60 min of treatment the temperature stops increasing and the pH value stabilises. This indicates that a time of 30 min of CO_2 sufficient to complete the carbonation reactions.

TG-DTA curves of carbonated samples are shown in Fig. 13. Peaks I and III in DTA curve respectively indicate the presence of hydrated calcium silicates and calcium carbonate. Samples C_AA3% and C_AA5% presents a mass loss in TG curve between around 300 °C and 500 °C. This mass loss confirms the presence of calcium acetate salts, as already observed in XRD pattern. The content of CO_2 from calcium carbonate, % $CO_{2,content}$, is calculated and reported in Table 8. The value has been corrected contribution of calcium acetate, as reported in Section 3.3, for samples C_AA1%, C_AA3% and C_AA5%. For these samples, the amount of calcium acetate, %Calc.Acet., was also quantified. $CO_{2,uptake}$ average values, calculated by means of Eq. 1, are expressed as a function of the acetic acid concentration in Fig. 14. It can be observed that the acidic conditions reduce the carbonation potential. This phenomenon can be attributed to a dual effect. The reaction of acetate ions with calcium ions results in the formation of calcium acetate, thereby reducing the availability of calcium to form calcium carbonate. The findings demonstrate a linear correlation between CO_2 uptake and acetic acid concentration, as well as a substantial linear correlation between calcium acetate and acetic acid concentration (see Table 8). Indeed, the utilisation of acetic

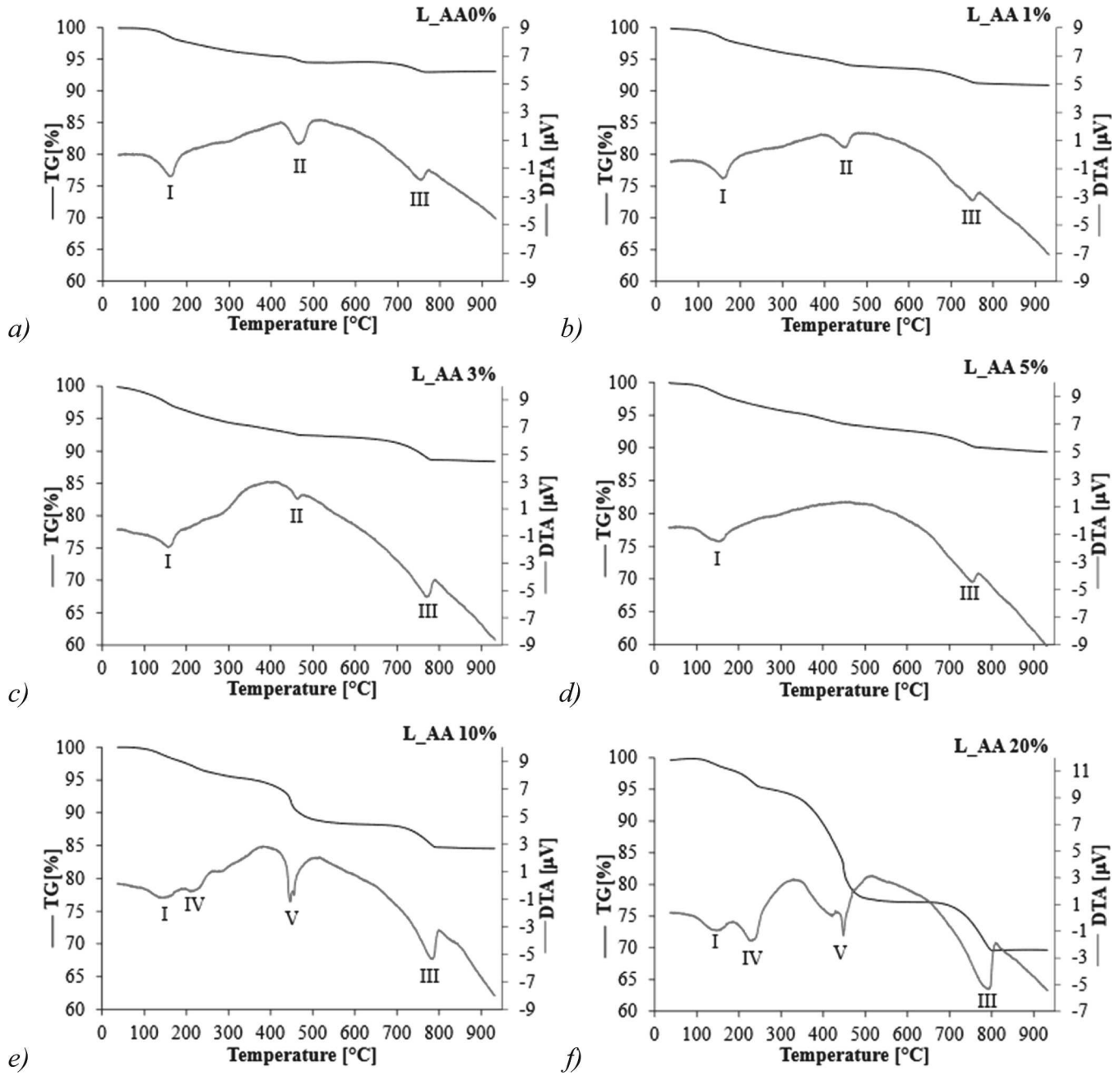


Fig. 9. DT-TGA curves of samples subjected to leaching tests.

acid has been demonstrated to result in a modest reduction in the absorption of carbon dioxide, accompanied by an augmentation in the presence of calcium acetate salt.

However, the C_AA3% and C_AA5% samples evidently demonstrate a reduction in reacted calcium when the contributions of carbonation and the formation of calcium acetate are summed ($\%CO_{2,content,tot}$ in Table 8). Consequently, in addition to the competition between carbonation and calcium acetate formation, a second effect exists that serves to reduce mineralisation efficiency. The lower pH associated with the use of acetic acid (see Fig. 11) creates less favourable conditions for carbonation reactions. Indeed, carbonation is promoted in an alkaline environment, as a lower pH value results in reduced dissolution of CO_2 into water [42].

4.3. Microstructure

Raw BOF slag particles exhibit a microstructure characterised by irregular shapes with sharp edges (Fig. 15a). The structure is created by the grinding process adopted to produce the powder particles. The size of the particle in the order of ten microns agrees with the granulometric analysis. Higher magnification shows few crystallised compounds on the flat surface of the particle (Fig. 15a). SEM images of carbonated samples, C_AA0%, are showed in Fig. 15c and Fig. 15d.

The surface of carbonated particles is completely covered by a layer of precipitates, corresponding to calcium carbonate presumably in the form of calcite, as indicated by the literature [14,18,20,54]. The image emphasises that the carbonation process significantly affects the structure of the particles, increasing the roughness of the surfaces.

The surface of particles carbonated after the leaching process in acidic conditions, C_AA3%, is also analysed. Similar to C_AA0%

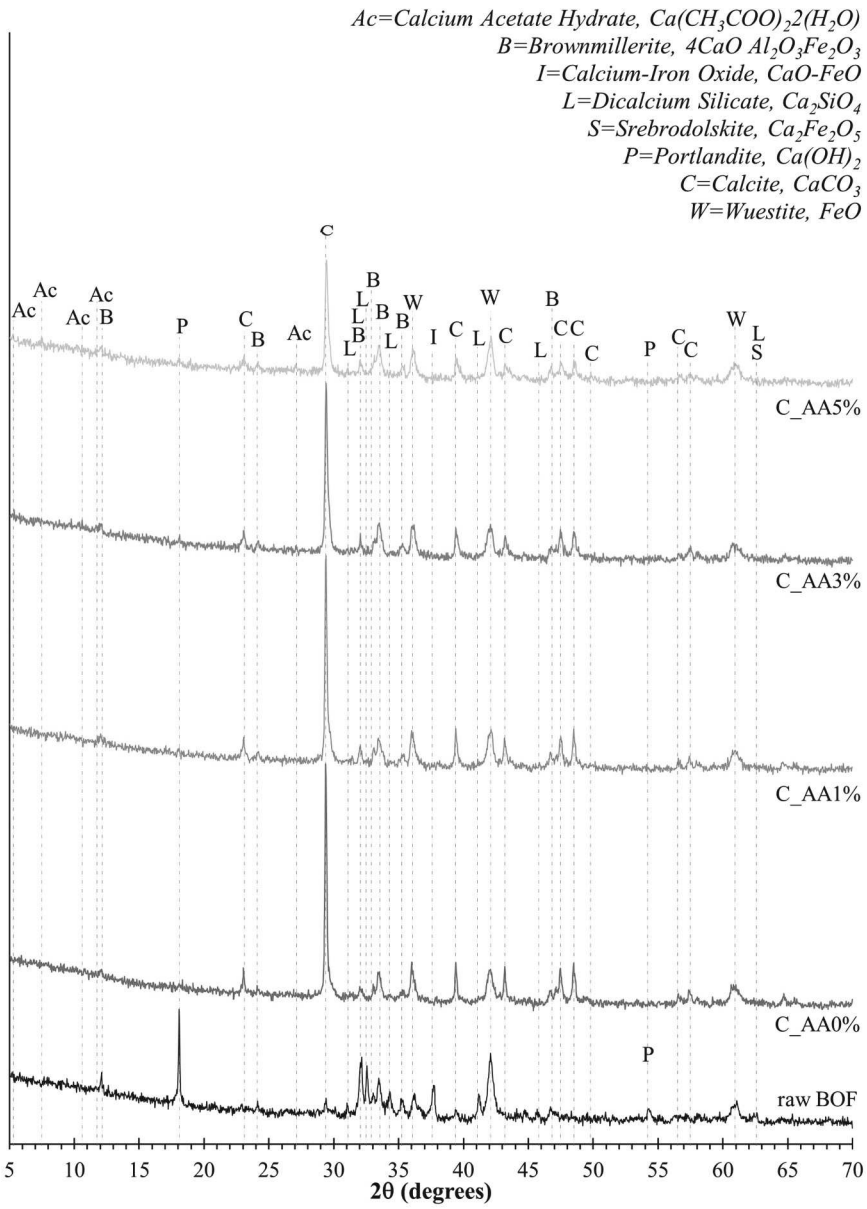


Fig. 10. XRD pattern of raw BOF and samples of carbonation tests.

particles, Fig. 15e shows the presence of a shell of calcium carbonate crystals that cover the surface of the particles. However, the distribution of these formations is less compact over the surface. At higher magnification, Fig. 15f, it is possible to observe that in some parts of the surface there is no evidence of calcium carbonate precipitation. This may be attributed to the leaching process that has released calcium ions from the particles before the carbonations, therefore leaving some parts, presumably rich in silica, not covered by carbonate precipitates.

EDX analysis provides a deeper understanding of the alterations in the morphology of the surface of the particles. Fig. 16, Fig. 17 and Fig. 18 respectively report EDX results of RawBOF, C_AA0% and C_AA3% samples. The elemental composition of the surface is investigated using maps created from a representative area of the particle. In addition, the elemental composition at specific points is reported. For each analysis, the EDX spectrum and the elemental composition, expressed as an atomic weight percentage, are reported. The RAWBOF sample map shows a significant presence of calcium and silica (Fig. 16b). This may be related to the calcium silicates identified by XRD analysis (Fig. 2). This evidence is corroborated by the elemental analysis of point 1 (Fig. 16c). The EDX analysis carried out on C_AA0% sample confirms the distributed presence of calcium carbonate (Fig. 17a). The elemental identification of the map (Fig. 17b) and of point 2 (Fig. 17c) shows a minor negligible presence of silica. This indicates that the carbonation creates a shell of calcium carbonate precipitate that impedes the availability of silica-bearing phases. Conversely, C_AA3% shows different formations on the surface (Fig. 18a). The map shows that some parts of the surface are characterised by the precipitation of calcium carbonate. The remaining regions are instead rich in silica, as indicated by the presence of the yellow colour. The elemental analysis of point 3, which is located in an area without calcium carbonate precipitates, shows a much higher silica concentration (Fig. 18c). Conversely, the elemental analysis of point 4, which is located in an area with calcium carbonate precipitates, shows negligible presence of silica (Fig. 18d).

The results show that the leaching treatment with acetic acid significantly affects the microstructure of the particles promoting the leaching of the calcium. Evidence of this can be seen in the change in the calcium-to-silica ratio. The Ca/Si ratio is equal to 6.3 at point 1 of the RAWBOF sample (Fig. 16c) decreasing to 0.18 at point 3 of the C_AA3% sample (Fig. 18c). This confirms that the acetic acid promotes calcium leaching, increasing the silica phase amount. Conversely, aqueous

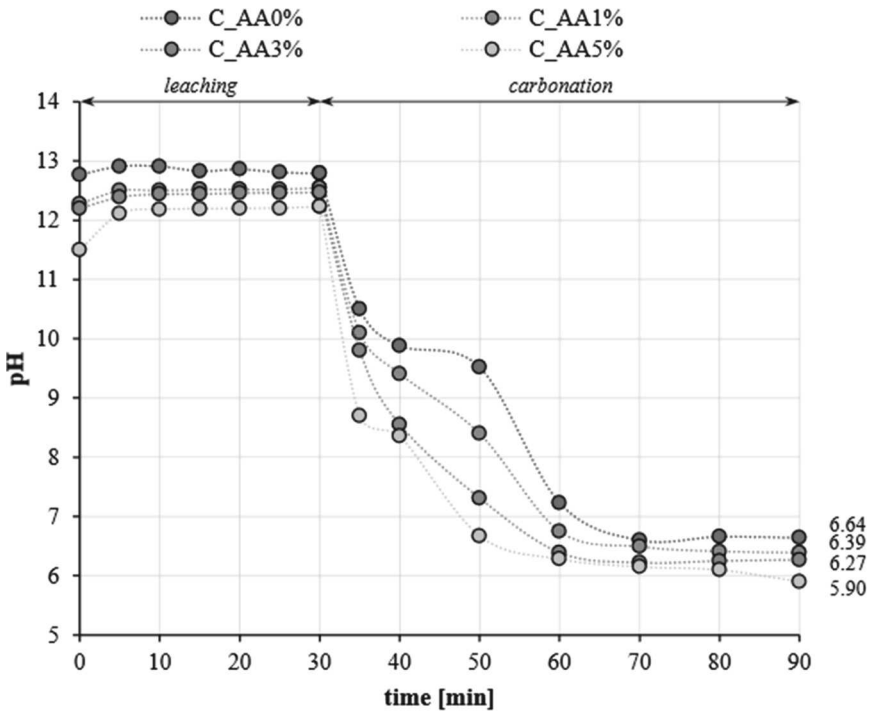


Fig. 11. pH evolution along the time of carbonation tests.

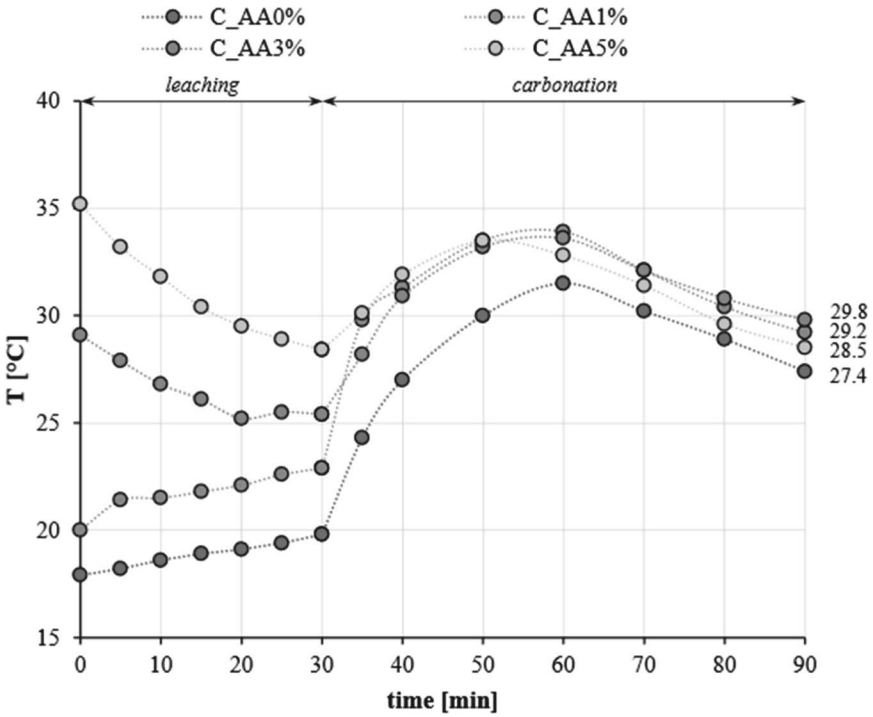


Fig. 12. Temperature evolution along the time of carbonation tests.

carbonation in the absence of acetic acid leads to the formation of a carbonate shell that completely covers the silica phases, impeding their availability in hydration processes (Fig. 17c).

4.4. Hydration mechanisms

Isothermal calorimetry analysis of cement blends including 20% of treated steel slag were carried out to investigate the influence of the mineralisation process on the hydration mechanisms. The evolution of the specific heat rate at early-stage, normalised with respect to the grams of cement, along the first 16 h of test are showed in Fig. 19. The curves are characterised by the acceleration period followed by a first peak associated with the dissolution of calcium silicates, C_3S, and precipitation of C-S-H. The second peak is associated with the dissolution of aluminate phases, and it is followed by the deceleration period [52,55]. The BOF20%_raw curve clearly shows that the presence of as-received

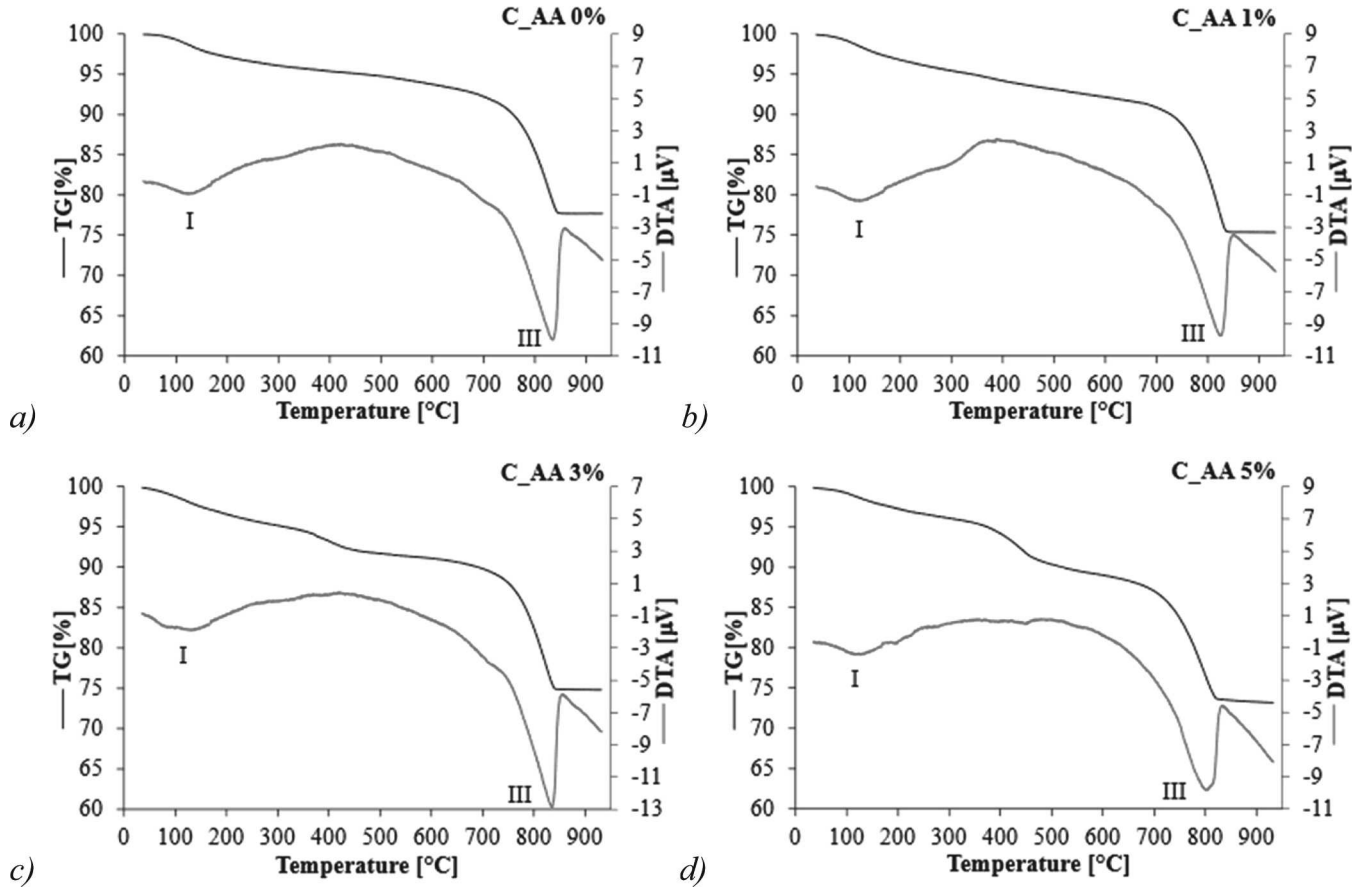


Figure 13. DT-TGA curves of samples subjected to carbonation tests.

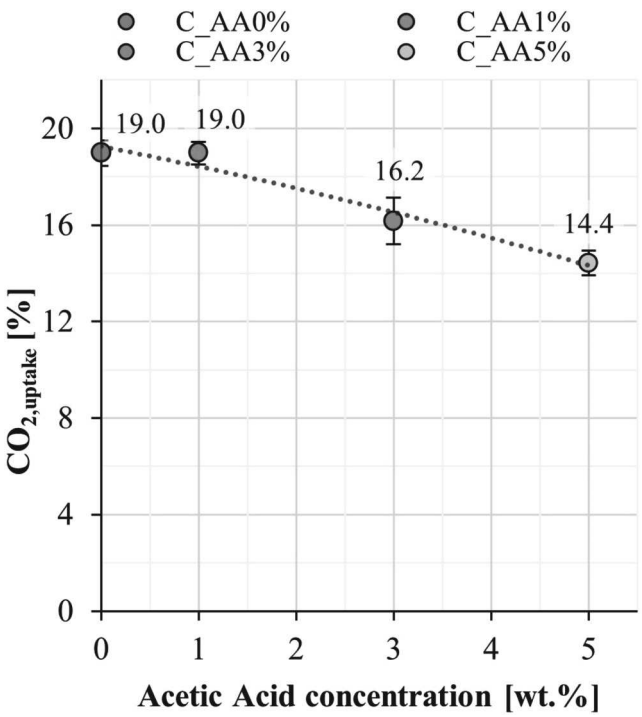


Fig. 14. $\%CO_{2,uptake}$ vs acetic acid concentration (trendline equation: $y = -0.03987x^2 - 0.78965x + 19.256$; $R^2 = 0.9654$).

steel slag in the blend significantly affects the heat rate slowing down the hydration process of the cement at early-stage. This finding aligns with similar studies in which 15–30% of cement is substituted with steel slag, and it may be attributed to the increase in Al concentration hindering C_3S dissolution, with consequent delay in the onset of the acceleration period [56,57]. This implies a higher hydration heat in the late-stage cement hydration, with total cumulative heat comparable with the value of the other series (Fig. 20). This is also emphasised by the values of the total cumulative heat normalised to the reference cement (Fig. 21).

The specific heat rate curves at early-hydration of carbonated samples show an acceleration period slightly anticipated with respect to reference cement. This acceleration may be attributed to nucleation sites provided by $CaCO_3$ particles which may promote the precipitation and growth of C-S-H [58]. However, it has been demonstrated that the nucleation effect is more pronounced with smaller carbonate particles formed during short carbonation duration (0–20 min). On the contrary, at high degree of carbonation (exceeding 40 min) the thicker outer layer of carbonates formed on the steel slag particles limits this effect and leads to minimal, or even negative, impact on the total hydration heat released [58]. The carbonated samples, although showing an earlier appearance of the first peak intensity compared to reference cement (see initial setting time in Fig. 22), do not show significant increase in total cumulative hydration heat values (Fig. 21). In addition, the carbonation does not seem to particularly affect the final setting time (Fig. 22). It can be concluded that the rougher surface of the carbonated particles generates a nucleation effect that is however limited by the high carbonation degree.

Regarding the use of acetic acid as leaching agent it is worth to emphasise that the specific cumulative heat curve of samples including the slag carbonated with the acid (BOF20%_C_AA1%, BOF20%_C_AA3%, and BOF20%_C_AA5%) is higher than the BOF20%_C_AA0%

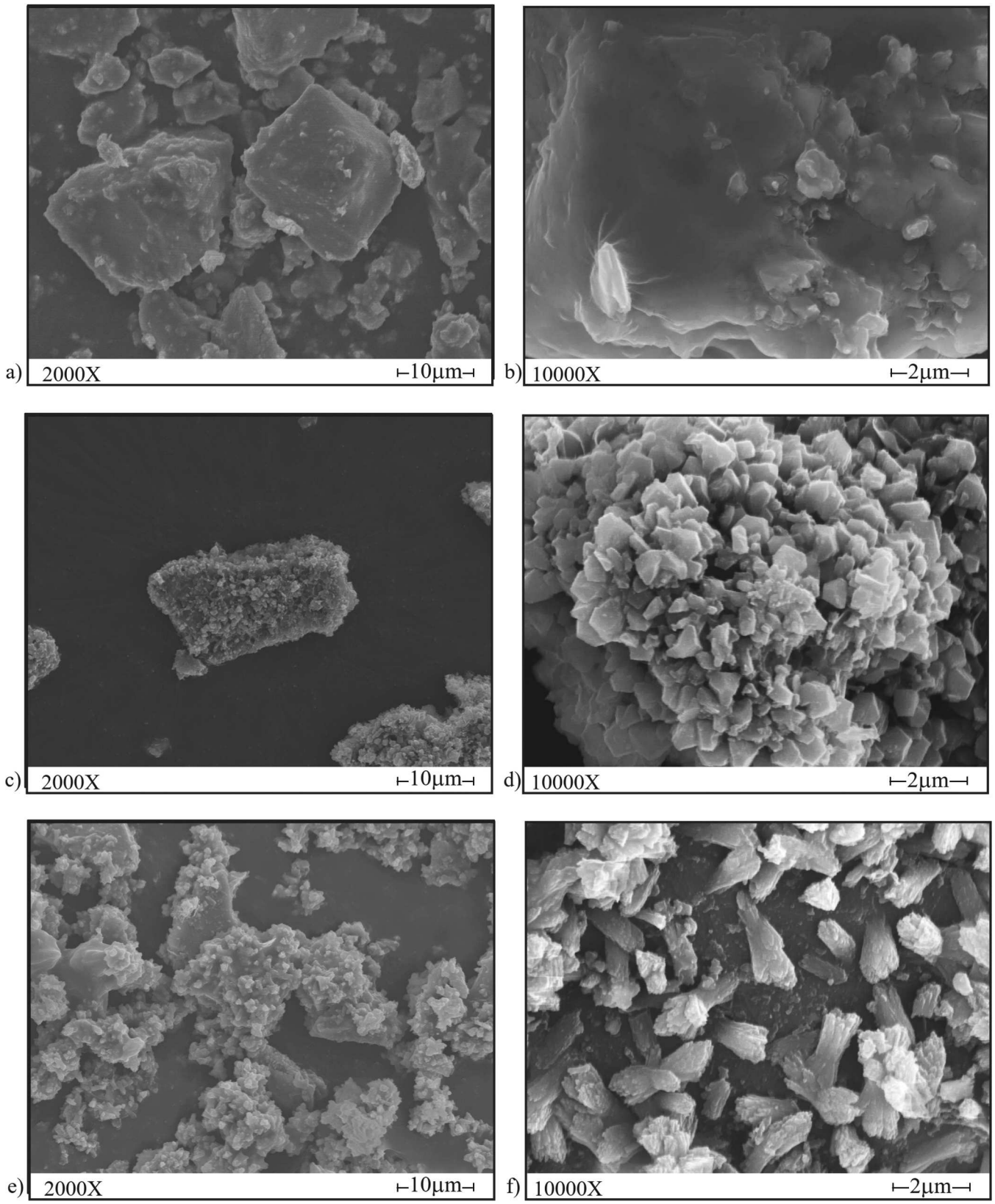


Fig. 15. SEM images of powders surface at 2000X magnification of a) RawBOF, c) C_AA0% and e) C_AA3% samples and at 10000X magnification of b) RawBOF, d) C_AA0% and f) C_AA3% samples.

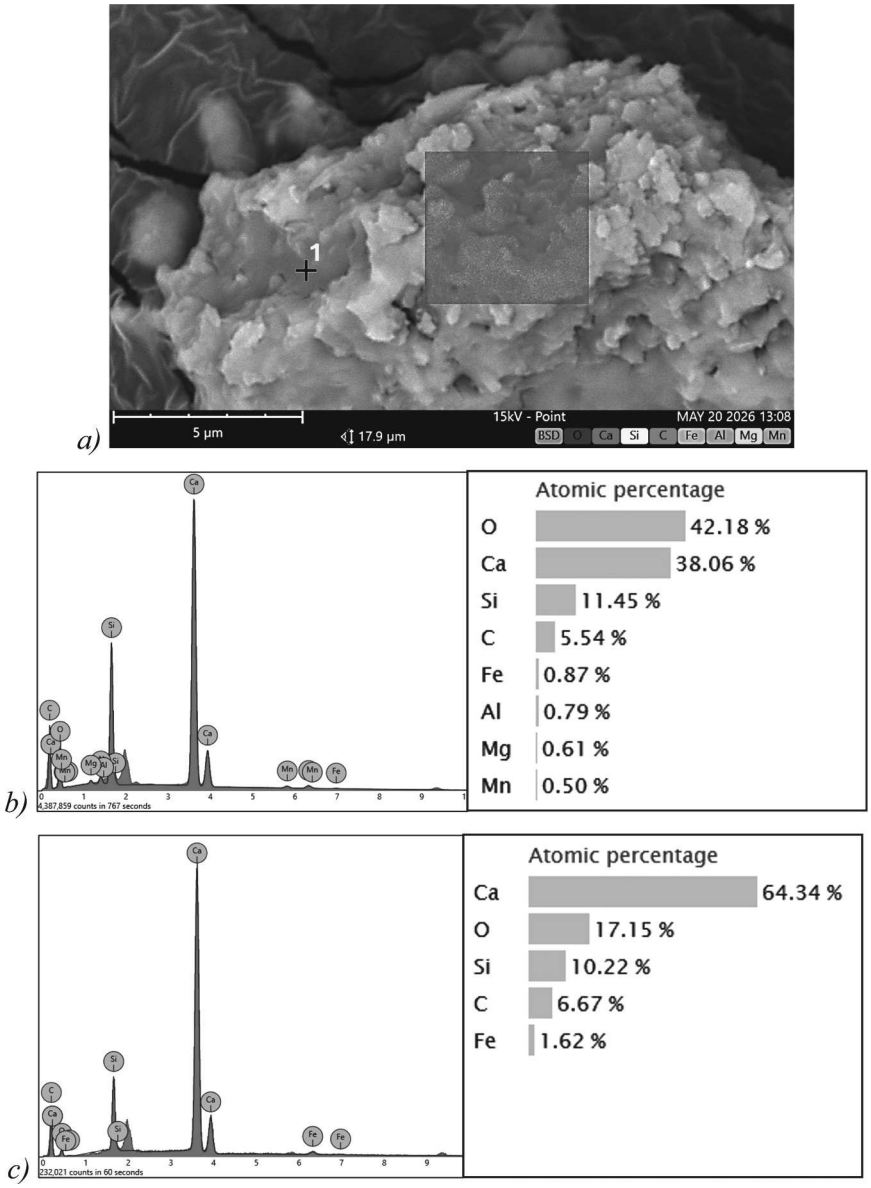


Fig. 16. a)SEM image of RAWBOF powder surface at 15000X magnification with map; b) EDX spectrum and elements identification of the map; c) EDX spectrum and elements identification of point 1.

sample (Fig. 20). In fact, while the normalised total specific heat of BOF20%_C_AA0% is only 4% higher than the reference cement sample, this increase is of around 10% in all the other samples carbonated with acetic acid. This outcome aligns with the fact that higher carbonation degrees may limit the hydration development. In fact, as shown in Fig. 14, the samples carbonated with acetic acid attained lower carbonation degrees.

Another fundamental aspect to understand the hydration mechanism is the effect of the carbonation treatment on the pozzolanic reactivity of the particles. The pozzolanic activity mainly consists in the formation of calcium-silicate-hydrate (C-(A)-S-H) gel from the reaction between Ca-leached alumina-silicate layer and portlandite. It has been observed that elevated carbonation degrees enhance the production of silica-rich phases with potential increase in pozzolanic reactivity [58]. In consistency with these observations, the portlandite consumption of the carbonated sample, C_AA0%, is higher with respect to the value exhibited by the raw BOF (Fig. 23). Similarly, an increase in bound water is also observed (Fig. 24). This is due to the formation of hydrated calcium silicates associated with the pozzolanic reactions. A further increase in pozzolanic reactivity is observed along with the increase in acetic acid adopted up to an acid concentration of 3%, despite the reduction in carbonation degree. This is explained with a detailed analysis of the microstructure of the carbonated particles. As known, in carbonated particles the silica-rich phases are encapsuled under a calcium carbonate barrier [14,18,20,54]. With the progression of the hydration process, the barrier layer may partially dissolve making the silica-rich phases available for pozzolanic reactions. The higher the carbonation degree, the higher the leached calcium and consequently the higher will be the silica content in the residual particles core. However, an opposite effect can be obtained with elevated carbonation degree. The formation of thick calcium carbonate barrier may impede the reaction of silicon and alumina ions from the particles core with portlandite, resulting in lower pozzolanic reactivity [58]. The higher pozzolanicity of C_AA1% and C_AA3% is, therefore, associated with the formation of a less compacted calcium carbonate layer. In fact, as observed in a representative image of C_AA3% carbonated surface (Fig. 15), the particle is not completely covered by calcium carbonate. This may reasonably promote the reaction of silica-rich phases, that are

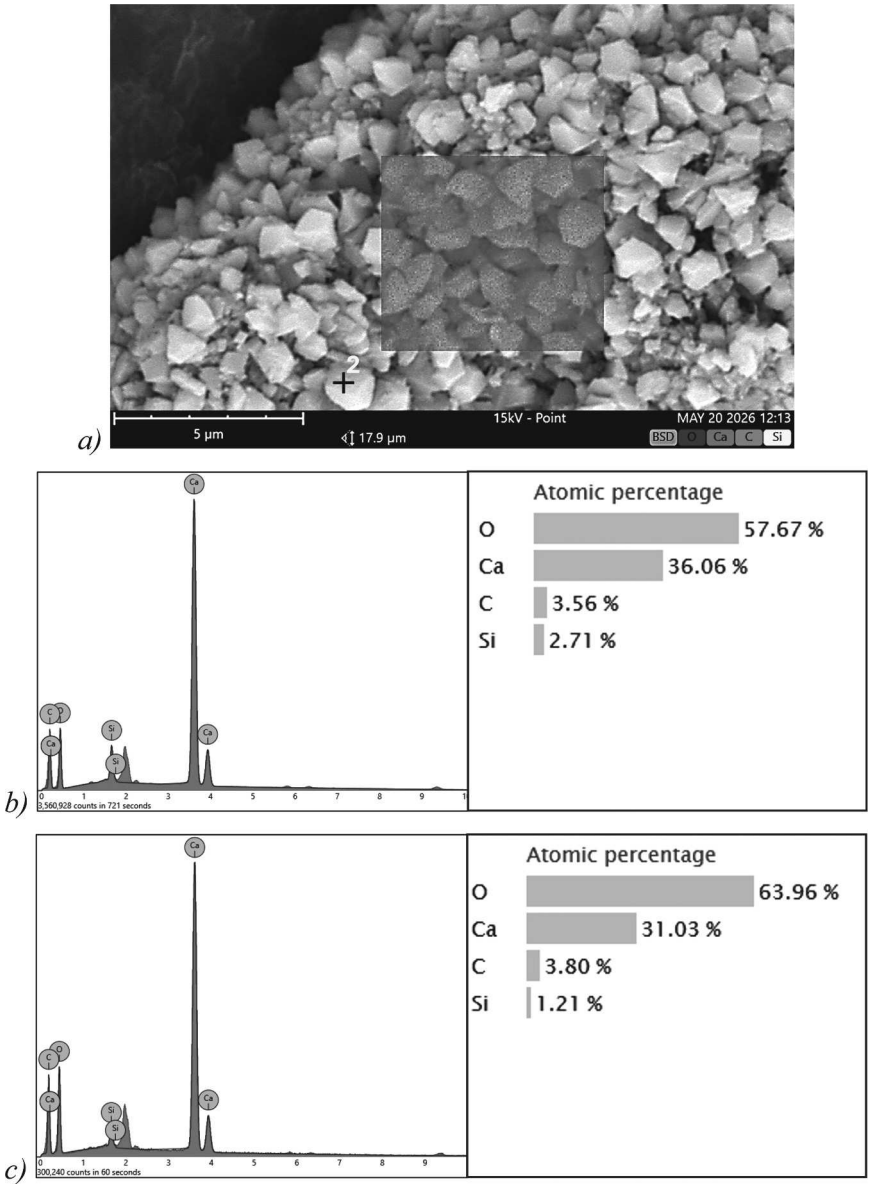


Fig. 17. a)SEM image of C_AA0% powder surface at 15000X magnification with map; b) EDX spectrum and elements identification of the map; c) EDX spectrum and elements identification of point 2.

present in the sample due to the calcium leaching associated with the use of acetic acid and to the carbonation reactions. As matter of fact, the partial reaction of calcium ions with acetic acid to form calcium acetate instead of calcium carbonate, promotes the availability of silica-rich phases, and at the same time it facilitates their reaction due to a less relevant $CaCO_3$ barrier layer.

The beneficial effect of the acidic process is however limited when high concentrations of acetic acid significantly lower the pH of the paste, creating not favourable conditions for the development of calcium silicate hydrates [34]. This justifies the reduction in portlandite consumption observed in C_AA5% sample that exhibited a pH value at the end of the carbonation process lower than 6 (Fig. 11). Based on the portlandite consumption and bound water results, the acetic acid concentration of 3% is optimal value for the hydration process. It is worth to observe that the evolution of bound water with acetic acid concentration (Fig. 24) follows the same trend of portlandite consumption (Fig. 23). This confirms that the effects of the carbonation in the hydration mechanism mainly affect the pozzolanicity of the particles that seems predominant compared to nucleation effect.

It is important to mention that a significant role in the hydration mechanisms is played by the calcium acetate. In fact, as demonstrated in the literature, the presence of calcium acetate releases Ca^{2+} ions that promote the hydration of calcium silicates [34,35]. This beneficial effect is not detected in portlandite consumption and bound water test, as the R^3 method is carried out with a mixture that does not include cement. It is evident that R^3 testing exclusively considers the beneficial contribution of reactivity in relation to alterations in the morphology of BOF particles. Conversely, the calorimetry test, conducted on cement blends, encompasses all the phenomena.

4.5. Mechanical strength

The behaviour at fresh state of cementitious mortar mixtures including 20% in weight of raw or treated BOF steel slag are showed in terms of spreading diameter in Fig. 25. The considered series are compared with the reference plain cement mortar, CEM100%_ref. The incorporation of raw BOF does not significantly affect the consistence of the mortar. On the contrary, the carbonated BOF steel slag significantly

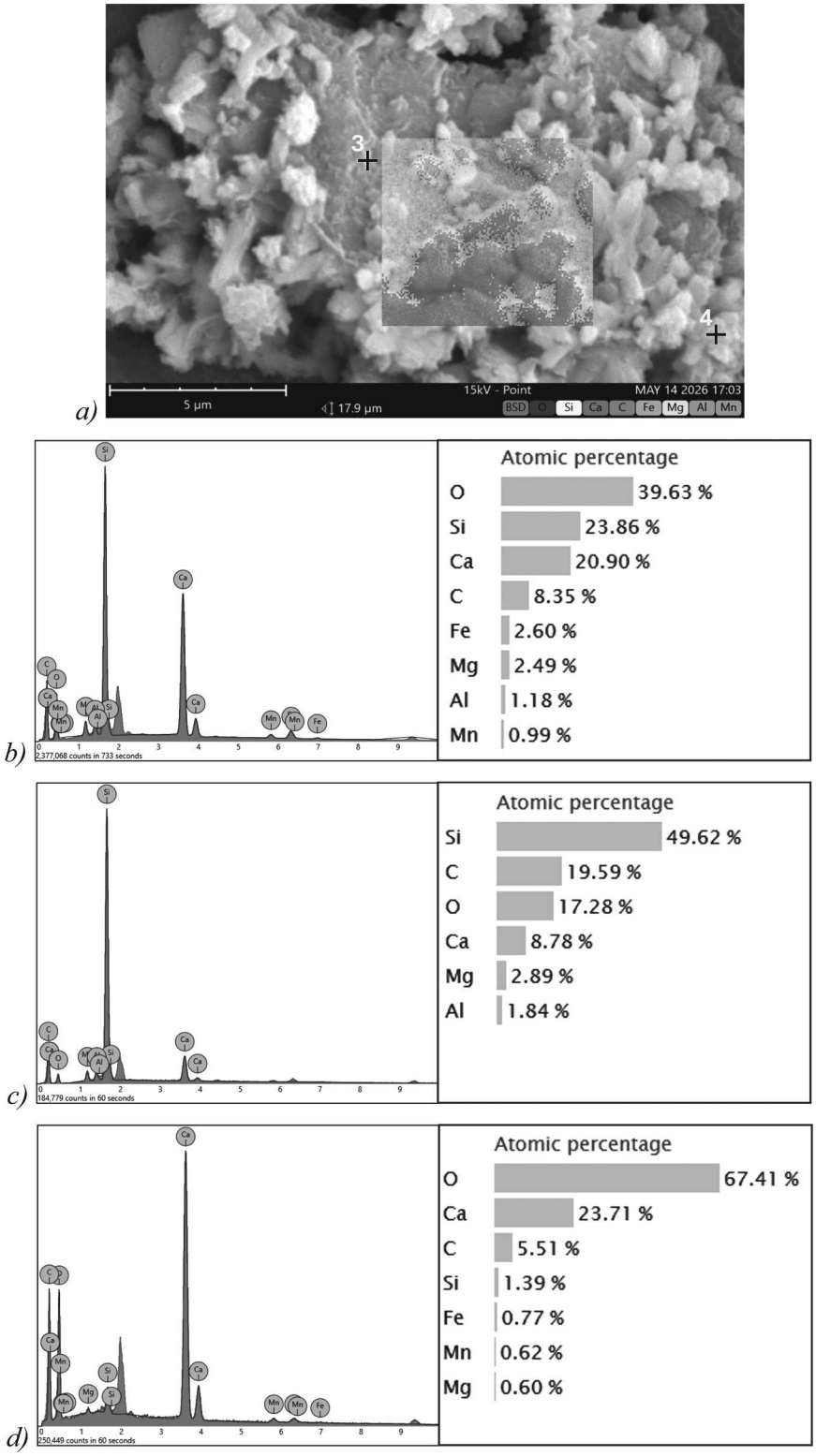


Fig. 18. a)SEM image of C_AA3% powder surface at 15000X magnification with map; b) EDX spectrum and elements identification of the map; c) EDX spectrum and elements identification of point 3; d) EDX spectrum and elements identification of point 4.

increases the consistence of the mixture (BOF20%_C_AA0%). This result aligns with the literature showing that the incorporation of carbonated steel slag increases the water demand of the mixture, and that this demand increases with dosage and CO_2 uptake [20,58]. This can be related to the higher specific surface area of the carbonated particles. The mineralisation causes rough structures on the particles surface (see Fig. 15) leading to higher yield stresses and viscosities and, subsequently, lower workability [58].

The series including BOF steel slag treated in acid acetic suspensions exhibit a higher flowability compared to the BOF20%_C_AA0% mixture. The same behaviour was observed in the literature with the addition of calcium acetate in the mixture [34]. The increased flowability of fresh

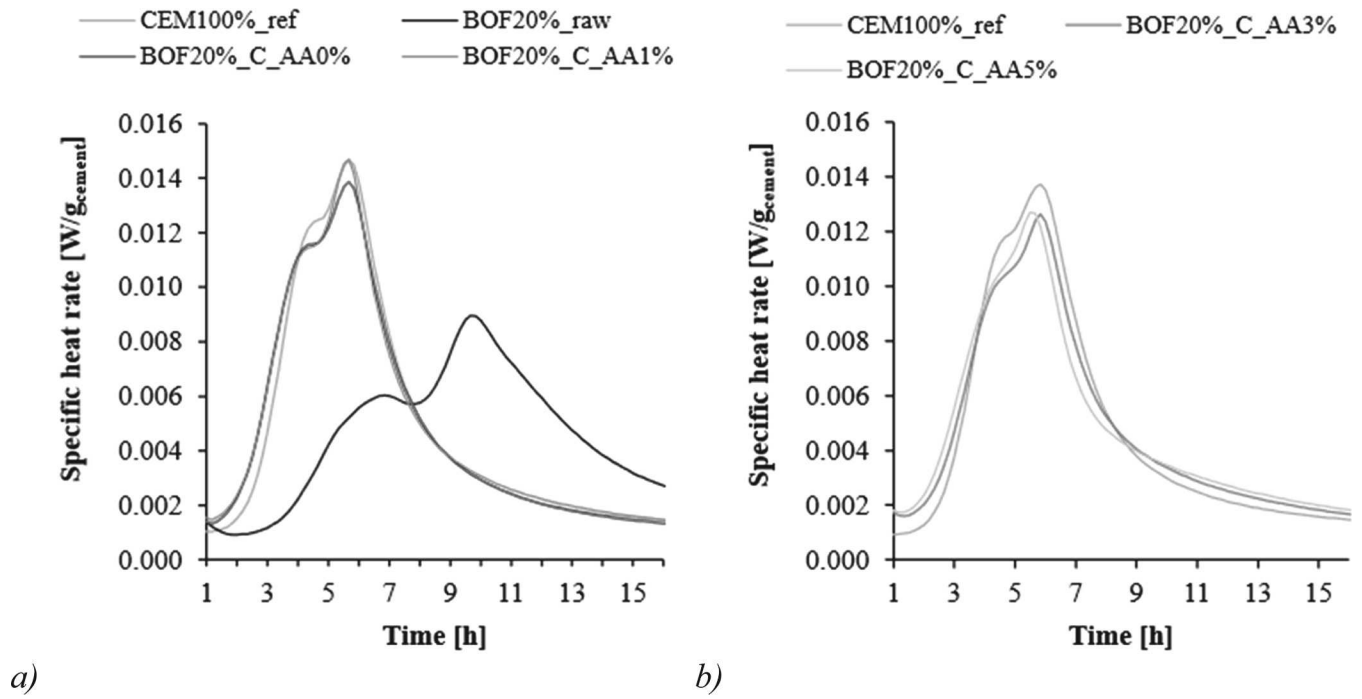


Fig. 19. Specific heat rate of samples by isothermal calorimetry (a) test1; b) test2).

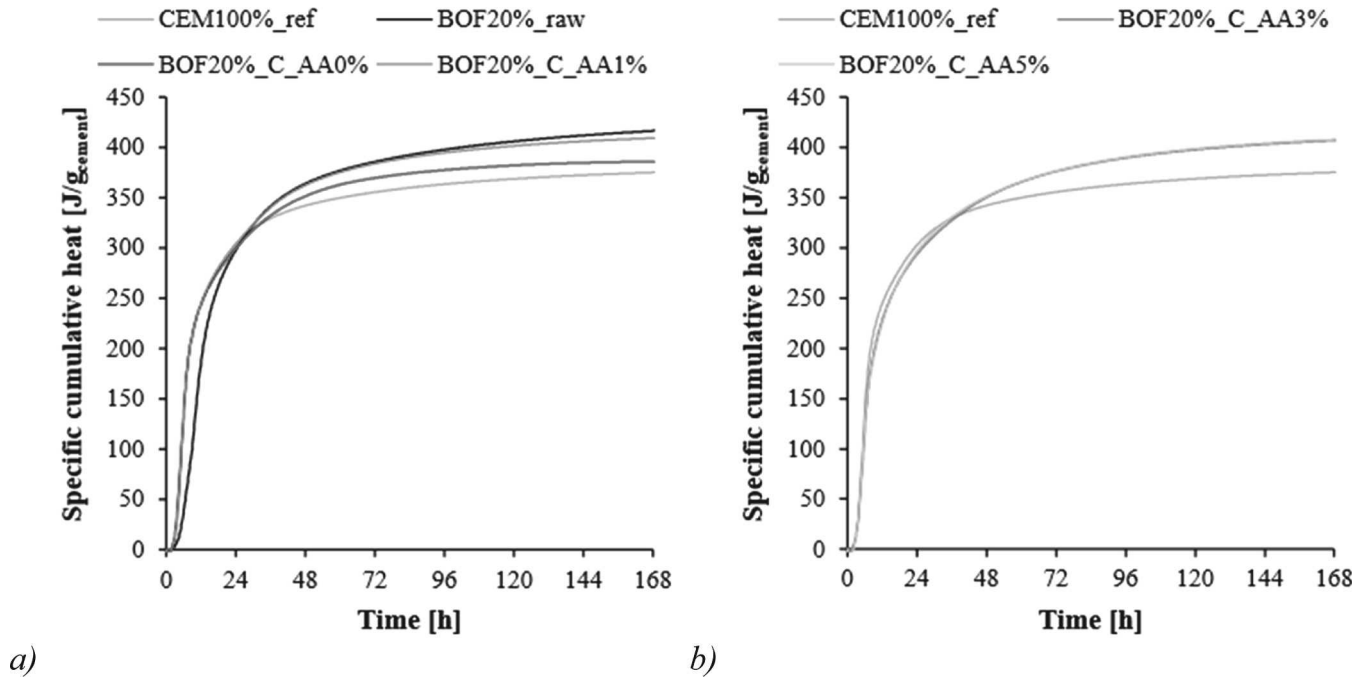


Fig. 20. Cumulative heat of samples by isothermal calorimetry (a) test1; b) test2).

mortars may be attributed to the adsorption of additional calcium ions from calcium acetate solutions onto cement particle surfaces, driven by the calcium concentration gradient between the solid and liquid phases, which enhances interparticle repulsion and dispersion [34]. Consequently, using acetic acid in the carbonation process mitigates the thickening effect associated with mineralisation. In fact, the reduction in the average spreading diameter decreases from about 20% in the BOF20%_C_AA0% series to about 10% in the BOF20%_C_AA3% and BOF20%_C_AA5% series.

Fig. 26 shows the average compressive strength at different times of curing of the mortar series. As expected, at all curing ages, the plain cement reference series, CEM100%_ref, exhibits the highest values, whilst the mortar incorporating the raw slag, BOF20%_raw, shows the lowest values. All the mortar incorporating carbonated slag show intermediate values, confirming that the mineralisation treatment enhances the properties of the steel slag. It is noteworthy that within the time interval 28–56 days, the BOF20%_raw series demonstrates the most significant increase in strength, while the remaining series of samples exhibit a substantial degree of hydration already after 28 days. This finding indicates that the BOF20%_raw hydration process is not

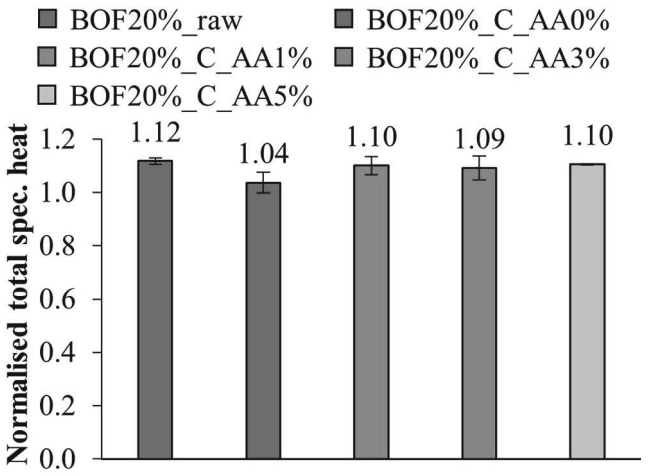


Fig. 21. Total specific heat normalized to the reference cement sample.

complete after 28 days of curing, thereby confirming that the incorporation of raw steel slag within the cement blend results in a delay in strength development. The use of carbonated steel slag mitigates this delaying effect [24].

Within the time interval 7–28 days, BOF20%_C_AA1% and BOF20%_C_AA3% series exhibited the highest increase in strength. This can be attributed to their enhanced pozzolanic reactivity, in consistency with the results in Fig. 23 and Fig. 24.

Fig. 27 shows the compressive strength activity index as function of the acetic acid concentration adopted in the treatment. The chart is reported at each curing time. The dashed line represents the average value associated with the BOF20%_raw samples. At a curing time of 3 and 7 days an increase in the activity index is observed with the carbonation (BOF20%_C_AA0%). However, the activity index value slightly decreases with the acetic acid concentration in the carbonation treatment.

At longer curing times, 28 and 56 days, a parabolic trend is observed with maximum value of the activity at an acetic acid concentration of about 3%. This trend is consistent with the results from the study of the hydration mechanisms. In addition, a significant role may also be attributed to the presence of calcium acetate in the carbonated powder that influences the strength development of the cement blend. In fact, based on the calcium acetate content in the treated powders (Table 8), the calcium acetate content in the mortar samples BOF20%_C_AA1% and BOF20%_C_AA3% is estimated respectively equal to around 0.1% and 1.0%. This finding aligns with the literature. Similar studies show 0.6% [35] and 1% (added as a 2% calcium acetate concentration solution with w/c of 0.5) [34] as optimum values of calcium acetate content in cement blends. The strength increase may be attributed to the presence of calcium ions and acetic acid radicals which contribute to the formation of complex that fill the internal pores of the cement paste during the hydration process [34]. As consequence, the hydration of C_2S, as well as pozzolanic reactions of active minerals are promoted [35].

The activity index shows a decrease, both at 28 and 56 days of curing, when higher concentrations of acetic acid are adopted during the carbonation treatment (see sample BOF20%_C_AA5% in Fig. 27). This trend, confirmed by similar studies [34,35], is related to the acidic conditions created using the acetic acid. In fact, lowering the pore solution pH has a negative effect on the calcium silicates hydration. In fact, as showed in Fig. 11, the sample with an acetic acid concentration of 5%, C_AA5%, attained the lowest pH after the carbonation, measuring below 6.

Overall, the findings in terms of mechanical strength corroborate the experimental evidence from the study of the hydration mechanisms presented in the previous section. Specifically, portlandite consumption (Fig. 23) and bound water (Fig. 24) tests, conceived to describe the hydration properties at a curing time equivalent to 28 days, provides a trend that is fully consistent with the activity index at 28 days (Fig. 27c). The overall findings confirm that the mineralisation process significantly affects the reactivity of steel slag particles increasing its pozzolanicity. Moreover, the use of adequate amount of acetic acid during the treatment, affects the microstructure of BOF particle surface and provides calcium acetate with consequent further enhancement of the cement blend hydration. It is important to note that while the effects of surface alteration can be observed through R^3 tests, the specific beneficial effect of calcium acetate in promoting calcium silicate hydration cannot be discerned from the results. Further research is required to explore this aspect, perhaps by mixing treated powder, purged from the salt, with pure calcium acetate.

It is worth to mention that the strength enhancement of strength observed in the BOF20%_C_AA3% specimen is accompanied by a decrease in CO_2 uptake of 2.8%. In contrast, the increase in strength of the BOF20%_C_AA1% specimen occurs without any reduction in CO_2 uptake. This consideration, in conjunction with the burdens associated with the use of acetic acid, should be considered when defining the optimum reagent content for industrial application of the process.

5. Comparison with the literature

5.1. Reactivity

The results in terms of bound water and portlandite consumption of all the series are compared with the reactivity values associated with

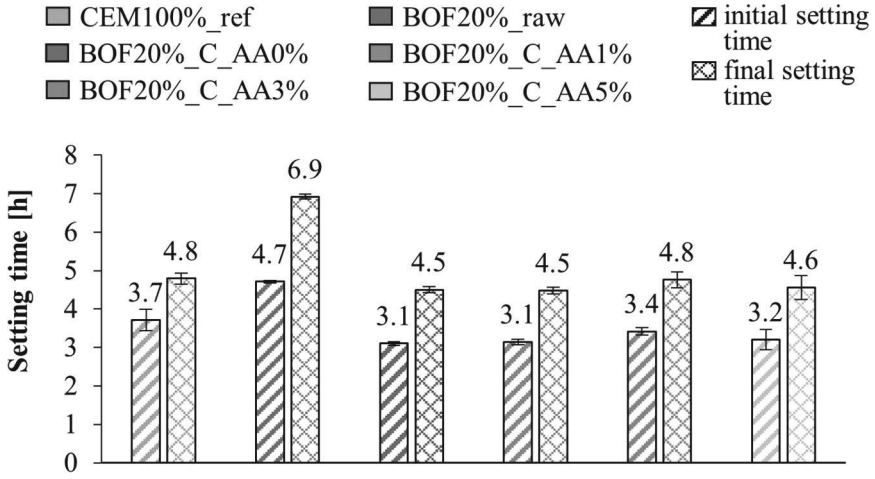


Fig. 22. Initial and final setting time obtained from calorimetry test.

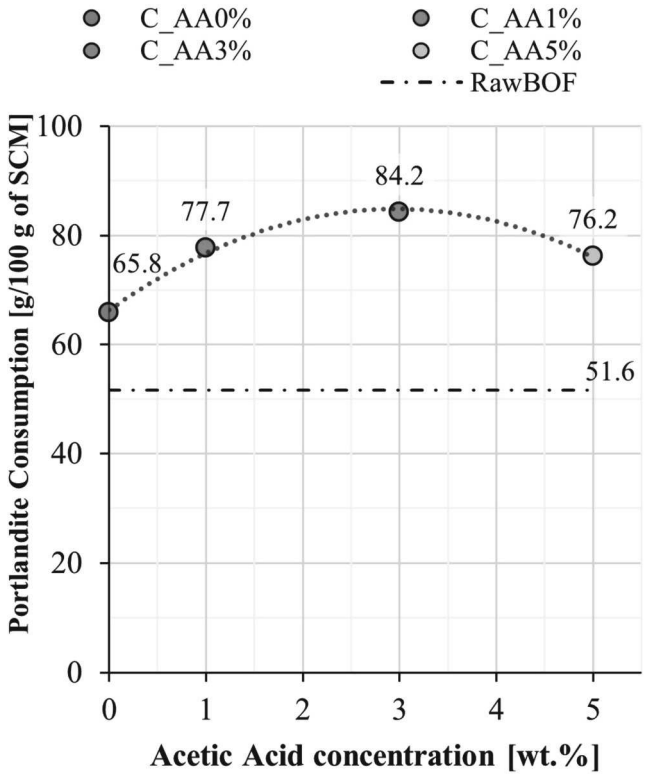


Fig. 23. Portlandite consumption vs acetic acid concentration (trendline equation: $y = -2.1146x^2 + 12.515x + 66.331$; $R^2 = 0.9905$).

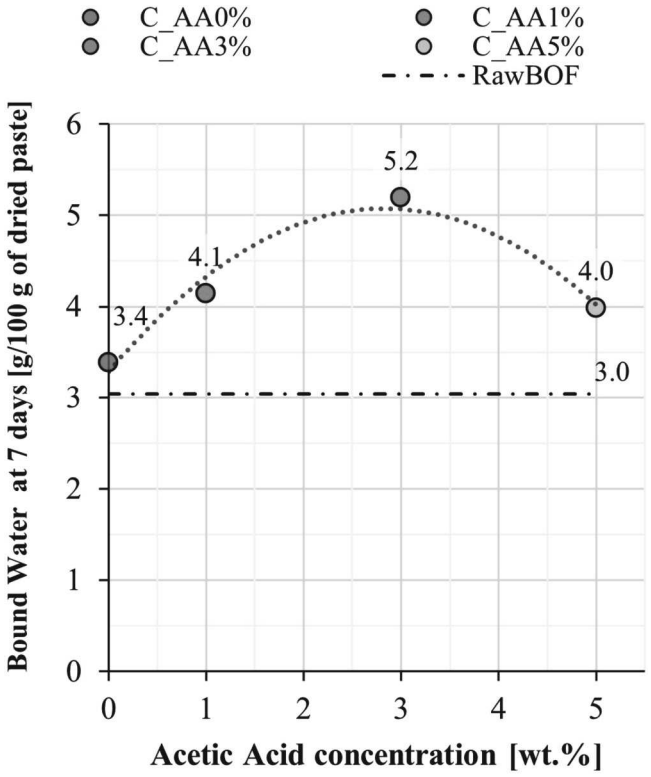


Fig. 24. Bound water vs acetic acid concentration (trendline equation: $y = -0.2236x^2 + 1.2651x + 3.2842$; $R^2 = 0.9635$).

conventional SCMs (Fig. 28 and Fig. 29). The dataset, described in Section 3.4, comprises various fly ashes, GGBS and natural pozzolan.

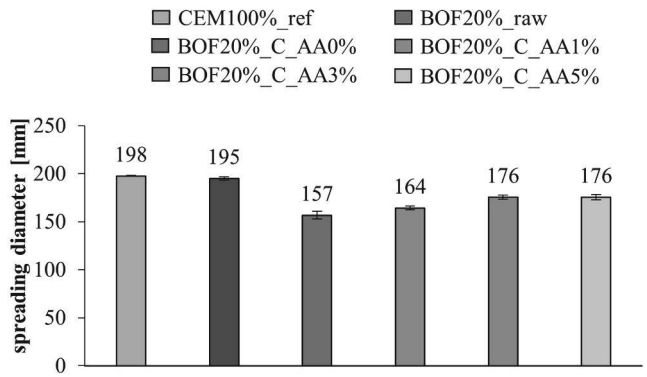


Fig. 25. Spreading diameter of the mortar series at fresh state.

Quartz is also considered as reference inert material. The slag adopted in the study, RawBOF, shows values higher than quartz. This indicate that the material is not characterised by a fully inert behaviour. However, comparing both bound water and portlandite consumption with the conventional SCMs, the RawBOF sample is collocated among the materials with low reactivity. Only few fly ashes exhibit lower values of bound water, but with higher portlandite consumption. This is related to the nature of the fly ash, typically characterised by amorphous silica-rich phases.

The carbonation treatment, in all the series, increase both bound water and portlandite consumption. This results in a reactivity behaviour in carbonated BOF steel slag that is more analogous to that of conventional SCMs. More in details, the series that showed the best performance, C_AA1% and C_AA3%, exhibit a behaviour comparable with GGBS. It is noteworthy that this by-product, similarly to fly ash, is extensively utilised in the production of standardised cement, such as CEM II. From this standpoint, the suggested mineralisation process enhances the value of BOF steel slag, rendering it suitable for utilisation as SCM.

5.2. Reduction in CO_2 emissions

A simplified assessment of the impact of the use of carbonated BOF slag in cement blends on the carbon footprint is herein proposed. The results are compared with the CO_2 emissions associated with the standardised cements. The dataset includes different cement types (CEM I, CEM II and CEM III) and of different strength class (42.5 and 52.5). The data are collected from Environmental Product Declarations (EPD) of cements produced in Europe. Table 9 reports the Global Warming Potential (GWP) representing the equivalent kg of CO_2 emitted for each ton of cement produced, and the cement replacement percentage (R), for each considered cement. It also reports the nature of the adopted cement replacement material, which are limestone, fly ash, blast furnace slag, ground granulated blasty furnace slag (GGBS), gypsum and other minor byproducts. More details concerning the dataset, including the cement company, the country and the year of production, the operator executing the EPD are reported in a previous study from the authors [16].

The carbon emissions associated with the cement blend adopted in the experimental activity of this study are calculated by subtracting the emissions related to the cement replacement (R) and to the CO_2 uptake of the adopted BOF slag to those of reference cement (avg $CO_{2,\text{emissions CEMI}}$) (Eq. 10).

$$CO_{2,emissions} = avgCO_{2,emissions\ CEMI}\left[\frac{kgCO_2}{ton\ of\ cement}\right] \bullet (1 - R) - CO_{2,uptake}\left[\frac{kgCO_2}{ton\ of\ carb\ slag}\right] \bullet R \quad (10)$$

It is worth to mention that this is a simplified approach that does not

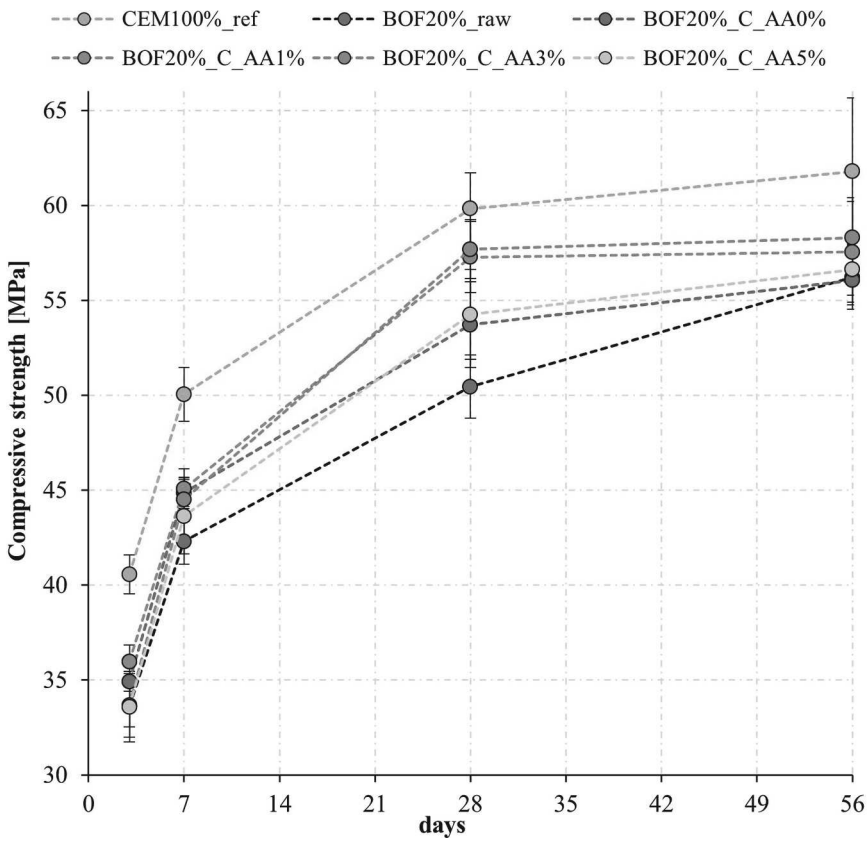


Fig. 26. Compressive strength development of the mortar series.

consider the emissions associated with the treatment of the slag and with the carbonation process. In fact, in a possible scenario in which the technology is implemented in a cement plant, these emissions are related to the specific site conditions. A more comprehensive life cycle assessment analysis is needed to take into account these aspects.

The emissions associated with the reference cement, are calculated as the average of the data reported in Table 9 referring to CEM I 52.5, and correspond to an average value of 791 kg CO_2 eq/ton of cement. The cement replacement, R, corresponds to 20%. CO_2 uptake values are those reported in Fig. 14.

Fig. 30 represents the relationship between the percentage of cement replacement and CO_2 emissions for the different classes of standardised cements considered in the study. Cements of type CEM I, notably not including SCMs, are characterised by the highest emissions. The other classes of cement considered shows a clear trend of reduction of the CO_2 emissions with the increase in cement substitution. The data point showing the lowest CO_2 emissions, associated with cement of typology CEM III, are characterised by percentage of cement substitutions higher than 80%. Two representative data of the study, BOF20%_raw and BOF20%_C_AA3%, are reported. The graph shows that the series adopted in the study aligns with the standard requirements of CEM II in terms of cement substitution percentage and CO_2 emissions.

Fig 31 shows the different strength classes of cement as function of the equivalent CO_2 emissions. The different region marked in the chart are defined considering the compressive strength requirements of cements of strength class of 425.5 and 52.5. All the data point associated with the series of samples considered in this study are reported. The chart shows that also in terms of strength class the series of samples can be associated with standardised cement of typology CEM II. However, while BOF20%_raw sample is associated with CEM II 42.5 type, all the samples including carbonated BOF also comply with the strength requirement of CEM II 52.5. More in particular, the series of samples showing the best strength performance (BOF20%_C_AA1% and BOF20%_C_AA3%), completely fit with their standard deviation in the region associated with cement of strength class 52.5. This is particularly important when comparing the performance of cement of type CEM I 52.5 having the same strength class but with a much higher carbon footprint.

All in all, the results show that the formulation adopted in the study provides cement blends that are comparable with standardised cements both in terms of cement substitution percentage and strength requirements. The aqueous carbonation process, improved by means of the acidic pre-treatment, strongly affects the overall performance of the material leading to an upgrade in terms of class strength from 42.5 to 52.5. At the same time, the gain in terms of carbon footprint is emphasised when comparing the optimised samples (BOF20%_C_AA1% and BOF20%_C_AA3%) with standardised cement with similar performance (i.e. CEM I 52.5).

6. Conclusions

The present study investigates the use of acetic acid in CO_2 mineralisation process to enhance the hydraulic reactivity of the carbonated BOF steel slag. With a holistic approach it analyses the leaching behaviour of the acidic suspension, the alterations in the chemical composition and in the morphology of the particles, the hydration mechanisms and the mechanical properties of cement blends incorporating the treated powder. Finally, a comparison with the extant literature and with standardised cement in provided. The main findings of the study are reported as follow:

– The leaching of BOF slag in acetic acid suspension induces calcium extraction from calcium silicates. The extraction capacity increases with the acid concentration up to a rate of 35.4% with 20 wt% acid content. The pH of the suspension is stabilised after 30 min of

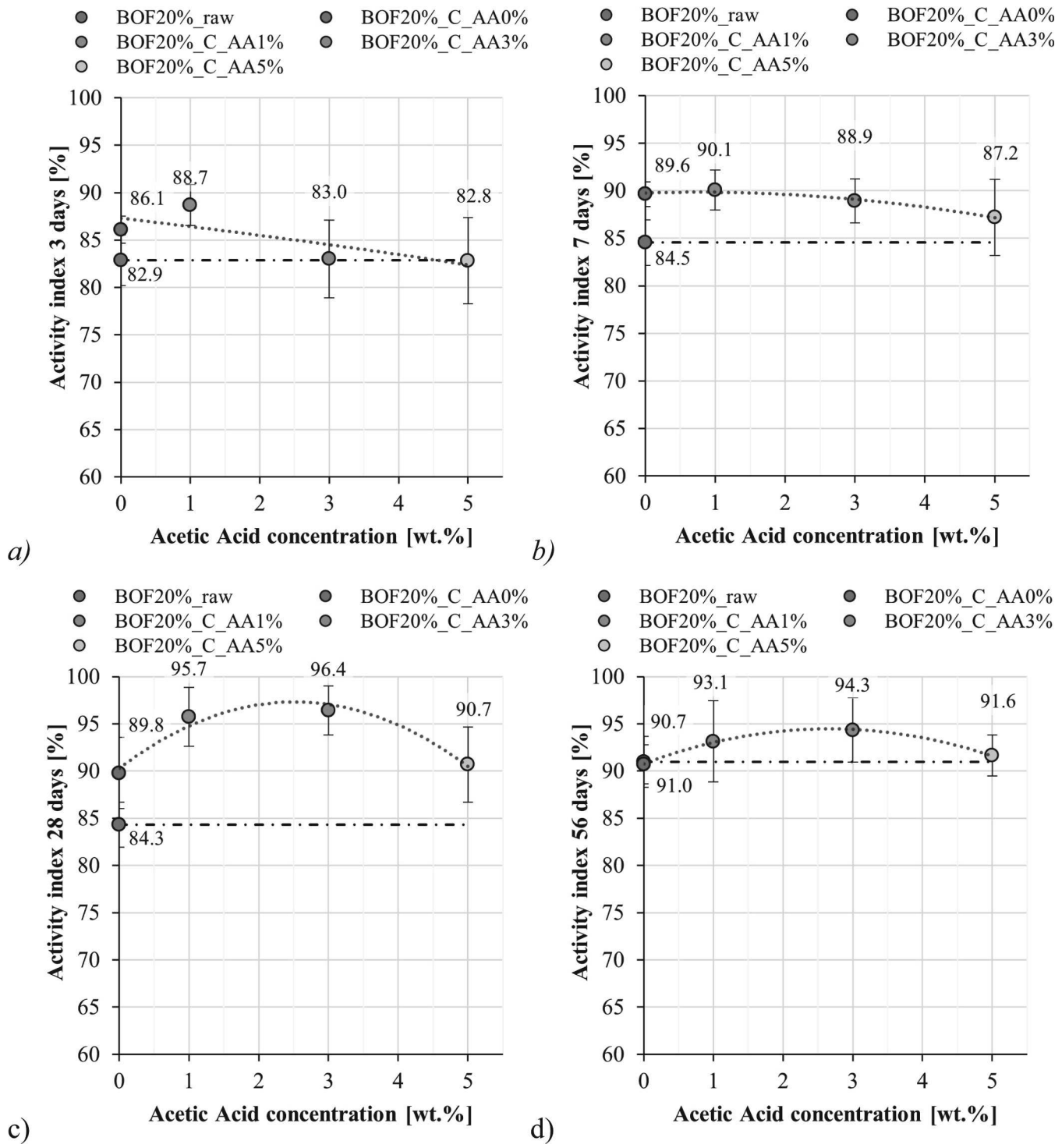


Fig. 27. Activity index of mortar series at curing age of: a)3 days (trendline equation: $y = -0.0273x^2 - 0.8491x + 87.304$; $R^2 = 0.613$); b)7 days (trendline equation: $y = -0.149x^2 + 0.2226x + 89.755$; $R^2 = 0.9813$); c)28 days (trendline equation: $y = -1.1088x^2 + 5.5847x + 90.282$; $R^2 = 0.9532$); d)56 days (trendline equation: $y = -0.5218x^2 + 2.7775x + 90.768$; $R^2 = 0.9975$).

treatment. Part of the extracted calcium reacts with acid to form calcium acetate salt.

- The carbonation process induces the conversion of dicalcium silicate and calcium hydroxide into calcium carbonate. In presence of acetic acid, part of the calcium reacts with the acid to form calcium acetate, with a content of the salt up to about 11% in sample with 5 wt% acetic acid concentration. As consequence, the carbonation degree linearly decreases with the acetic acid content. Despite this, the CO_2 uptake, of approximately 19% in the sample carbonated without acetic acid, remains relevant with a value of approximately 14.4% in samples carbonated with 5 wt% acetic acid concentration.
- The carbonation process significantly alters the microstructure of the particles with the formation of calcium carbonate precipitates on the surface of the particles. The distribution of the carbonate layer results less compact over the surface in samples carbonated in presence of acetic acid. This indicates that the leaching process promotes the

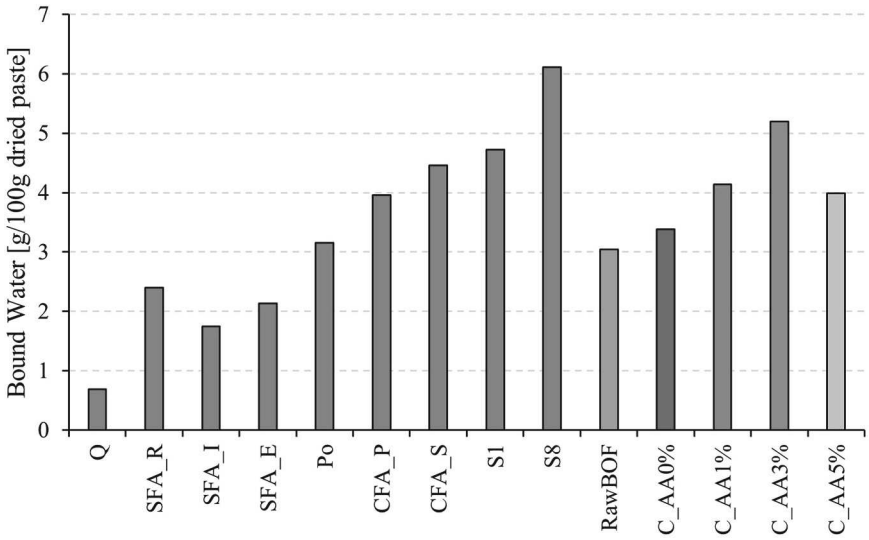


Fig. 28. Comparison with literature data in terms of Bound Water.

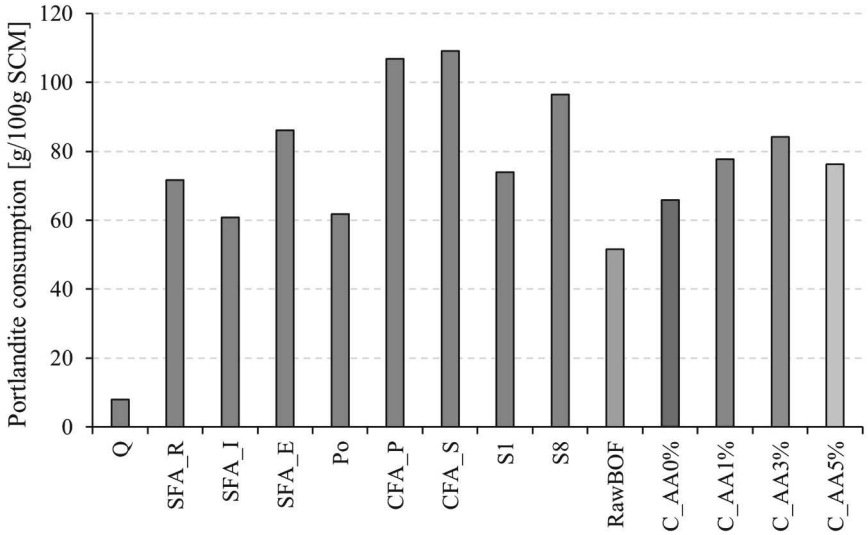


Fig. 29. Comparison with literature data in terms of Portlandite Consumption.

extraction of calcium from the particles before the carbonation, significantly reducing the Ca/Si ratio on the particle surface.

- The acetic acid affects the hydration heat of cement blends incorporating the treated powder with a slight increase in cumulative heat compared to the carbonated BOF without acid. Similarly, beneficial effects are observed in terms of bound water and portlandite consumption. These parameters are related to the acetic acid content following a parabolic trend with maximum value at a concentration of approximately 3 wt%. This can be associated with the to partial reaction of calcium with acetic acid to form calcium acetate instead of calcium carbonate, that leads to the formation of less compacted calcium carbonate layer. This promotes the reactivity of the silica-rich phases.
- The beneficial effect in terms of hydration is limited at elevated acetic acid concentrations, as the associated decrease in pH generates conditions that are not favourable to the formation of calcium silicate hydrates. This is consistent with the reduced portlandite consumption observed in the C_AA5% sample, which exhibited a final pH below 6 after the carbonation process.
- The acetic acid strongly affects the mechanical behaviour of the treated powder adopted to produce mortar samples in cement blends with 20% substitution. A parabolic trend, similar to those observed from the study of the hydration mechanisms, is observed with compressive strength activity index at 28 days that achieves the maximum value in BOF20%_C_AA3% sample. The presence of calcium acetate, equal to approximately 1% in BOF20%_C_AA3% sample, showed to contribute to the hydration enhancement of the cement blend.
- The comparison with the literature shows that the treated powders exhibit portlandite consumption and bound water values in line with the values of conventional SCMs. In fact, the cement blends incorporating the carbonated BOF are comparable with standardised cements in terms of both cement replacement percentage and strength requirements. All the samples incorporating carbonated BOF comply with the strength requirement of CEM II 52.5.

The overall results show a clear correlation among CO_2 uptake, bound water, portlandite consumption and mechanical strength, clearly defining the beneficial role of the acetic acid. Based on the findings, an acetic acid concentration of 3 wt% may be considered an optimised amount for the hydration process. This leads to a compressive strength activity index of approximately 96.4% at 28 days, while adopting a

Table 9
Standardised cement dataset (extracted from [16]).

CEM type	R [%]	GWP [kg CO_2 eq]
CEM I 52.5	Other < 5%	773
	Limestone < 5%	681
	Other < 0.5%	
	Other < 5%	803
	Other < 5%	664
	Other < 5%	793
	Other < 5%	960
	Other 2.57%	864
CEM II 52.5	Limestone 6−20%	633
	Others < 5%	
	Limestone 5−15%	620
	Slag 5−15%	
	Others < 0.5%	
	Others 0−5%	636
	Fly ash 6−20%	
	Blast furnace slag 21−35%	641
	GGBS 31.4%	564
	Limestone 9.5%	761
	Others 4.8%	
	GGBS 21−35%	524
CEM II 42.5	Gypsum 0−5%	662
	Fly ash 6−20%	
	10.3%	527
	10.5%	709
	4.8%	788
	Slag 21−35%	656
	Byproducts 6.5%	741
	Byproducts 6.1%	672
CEM III 42.5	Byproducts 38%	561
	Slag 63.5%	392
	Clinker 32%	
	Slag 63.1%	379
	Clinker 31.5%	
	Slag 77%	272
	BF 36−65%	382
	Slag 50%	358

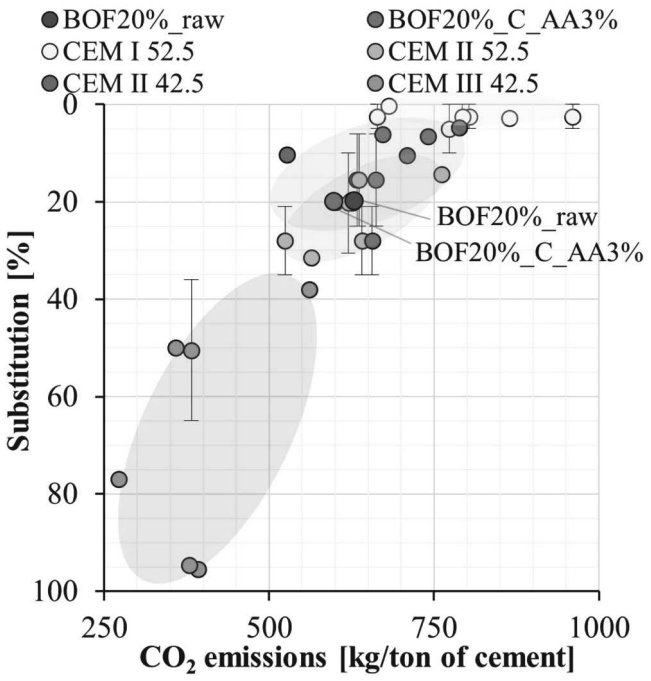


Fig. 30. CO_2 equivalent emissions of different cement types based on their replacement rate integrated with the results of this study.

carbonated BOF with CO_2 uptake of approximately 16.2%.

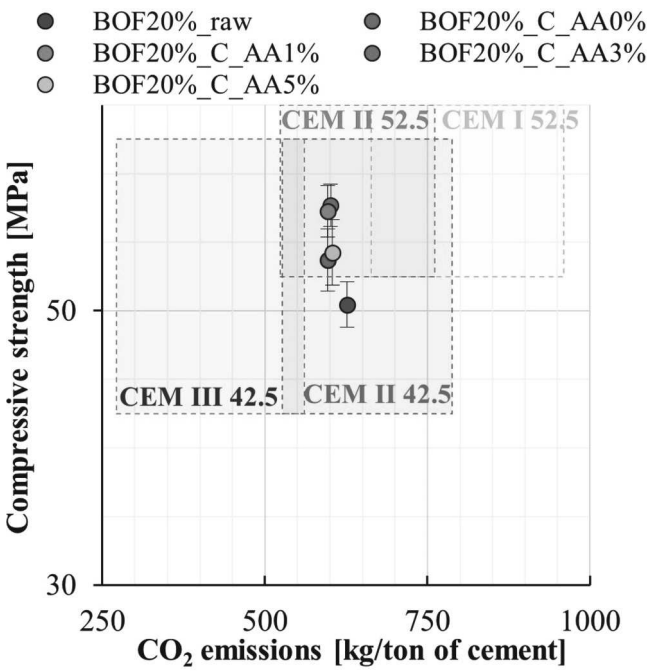


Fig. 31. CO_2 equivalent emissions of different cement types based on their compressive strength integrated with the results of this study.

Furthermore, the use of acetic acid showed to strongly enhance the reactivity of the treated powder, with considerable increase of the compressive strength activity index at 28 days with respect to blends incorporating raw BOF and carbonated BOF without acetic acid, attaining values of 84.3% and 89.8% respectively.

Nevertheless, further investigation is needed to improve the overall efficiency of the process. In fact, while part of the acetic acid reacts within the process to form calcium acetate employed in the cement blend, the remaining chemical is wasted during the centrifuge treatment. In this regard, solutions are needed to implement the recovery of the chemical and to promotes its reuse in the process.

Furthermore, the investigation of the individual role of calcium acetate in the strength development remains a limitation of the study. Further research is required to investigate this aspect, for example by adding pure calcium acetate to the treated slag purged from the salt formed during the carbonation.

The findings of the study, showing a significant enhancement of the conventional aqueous carbonation process, paves the way for possible industrial applications in cement industry to produce innovative blends with reduced environmental impact. In this regard, life cycle assessment analysis is envisaged to quantify the overall environmental benefits of the proposed process.

CRediT authorship contribution statement

Pedro Humbert: Writing – review & editing, Validation, Supervision, Conceptualization. **Paola Palmero:** Writing – review & editing, Supervision, Project administration, Conceptualization. **Giuseppe Ferrara:** Writing – original draft, Methodology, Investigation, Formal analysis, Conceptualization.

Declaration of Competing Interest

The authors declare that they have no known competing financial interests or personal relationships that could have appeared to influence the work reported in this paper.

Acknowledgements

The authors gratefully acknowledge the Safety of Infrastructures and Constructions (SISCON) laboratory for providing the instrumentation for thermal analysis.

Data availability

Data will be made available on request.

References

[1] K.M. Ripley, F.H. Saadi, Z.L.H. Burke, Cost-motivated pathways towards near-term decarbonization of the cement industry, RSC Sustain. 3 (1) (2025) 255–263, https://doi.org/10.1039/D4SU00590B.
[2] E. Jessa, A. Ajidahun, Sustainable practices in cement and concrete production: reducing CO_2 emissions and enhancing carbon sequestration, World J. Adv. Res. Rev. 22 (2) (2024) 2301–2310, https://doi.org/10.30574/wjarr.2024.22.2.1412.
[3] International Energy Agency. Cement, IEA; 2020 https://www.iea.org/energy-system/industry/cement.
[4] P.J. Monteiro, S.A. Miller, A. Horvath, Towards sustainable concrete, Nat. Mater. 16 (7) (2017) 698–699, https://doi.org/10.1038/nmat4930.
[5] Cembureau, The European cement association - 2019 Activity Report, 2019. https://cembureau.eu/media/clkdda45/activity-report-2019.pdf.
[6] B. Lothenbach, K. Scrivener, R.D. Hooton, Supplementary cementitious materials, Cem. Concr. Res. 41 (12) (2011) 1244–1256, https://doi.org/10.1016/j.cemconres.2010.12.001.
[7] U.N. Environment, K.L. Scrivener, V.M. John, E.M. Gartner, Eco-efficient cements: potential economically viable solutions for a low-CO_2 cement-based materials industry, Cem. Concr. Res. 114 (2018) 2–26, https://doi.org/10.1016/j.cemconres.2018.03.015.
[8] F. Bonfante, G. Ferrara, P. Humbert, D. Garufi, J.M.C. Tulliani, P. Palmero, CO_2 sequestration through aqueous carbonation of electric arc furnace slag, J. Adv. Concr. Technol. 22 (4) (2024) 207–218, https://doi.org/10.3151/jact.22.207.
[9] F. Bonfante, P. Humbert, J.M. Tulliani, P. Palmero, G. Ferrara, CO_2 uptake of cement by-pass dust via direct aqueous carbonation: an experimental design for time and temperature optimisation, Mater. Struct. 57 (8) (2024) 181, https://doi.org/10.1617/s11527-024-02457-0.
[10] A.F. Mohammad, M. El Gamal, N. Mousa, A.H. Al-Marzouqi, From carbonation chemistry to structural performance: Sulfur concrete from brine salts and carbide lime, Appl. Mater. Today 48 (2026) 103066, https://doi.org/10.1016/j.apmt.2025.103066.
[11] F. Bonfante, G. Ferrara, J.M. Tulliani, P. Palmero, A comprehensive review of direct aqueous mineral carbonation of industrial wastes using principal component analysis, J. Sustain. Cem. -Based Mater. (2025) 1–25, https://doi.org/10.1080/21650373.2025.2567002.
[12] Y.R. Yi, Y. Lin, Y.C. Du, S.Q. Bai, Z.L. Ma, Y.G. Chen, Accelerated carbonation of ladle furnace slag and characterization of its mineral phase, Constr. Build. Mater. 276 (2021) 122235, https://doi.org/10.1016/j.conbuildmat.2020.122235.
[13] H. Wang, G. Zhou, Y. Mu, M. Zhang, M. Guo, Enhanced carbon dioxide sequestration and Cr detoxification: Direct carbonation of AOD slag with additives under ambient conditions, J. Clean. Prod. 443 (2024) 141181, https://doi.org/10.1016/j.jclepro.2024.141181.
[14] G. Ferrara, A. Belli, A. Keulen, J.M. Tulliani, P. Palmero, Testing procedures for CO_2 uptake assessment of accelerated carbonation products: experimental application on basic oxygen furnace steel slag samples, Constr. Build. Mater. 406 (2023) 133384, https://doi.org/10.1016/j.conbuildmat.2023.133384.
[15] F. Bonfante, G. Ferrara, P. Humbert, J.M. Tulliani, P. Palmero, Direct aqueous mineralization of industrial waste for the production of carbonated supplementary cementitious materials. In International RILEM Conference on Synergising expertise towards sustainability and robustness of CBMs and concrete structures (June), Springer Nature Switzerland, Cham, 2023, pp. 581–592, https://doi.org/10.1007/978-3-031-33187-9_54 (June).
[16] F. Bonfante, G. Ferrara, P. Humbert, D. Garufi, J.M. Tulliani, P. Palmero, Aqueous carbonation of EAF steel slag to produce supplementary cementitious material: effects on mineral composition, hydration reactivity and mechanical properties, Constr. Build. Mater. 479 (2025) 141361, https://doi.org/10.1016/j.conbuildmat.2025.141361.
[17] F. Bonfante, P. Humbert, D. Garufi, J.M. Tulliani, P. Palmero, G. Ferrara, Aqueous carbonation of cement bypass dust for reuse in cement: potassium chloride removal, hydration reactivity and mechanical properties, Constr. Build. Mater. 506 (2026) 145004, https://doi.org/10.1016/j.conbuildmat.2025.145004.
[18] Y. Fang, W. Su, Y. Zhang, M. Zhang, X. Ding, Q. Wang, Effect of accelerated precarbonation on hydration activity and volume stability of steel slag as a supplementary cementitious material, J. Therm. Anal. Calorim. 147 (11) (2022) 6181–6191, https://doi.org/10.1007/s10973-021-10914-z.
[19] Z. Jiang, X. Ling, Q. Liu, H. Song, K. Schollbach, H.J.H. Brouwers, Basic oxygen furnace (BOF) slag cementitious binder activated by Na4EDTA, Cem. Concr. Res. 198 (2025) 107983, https://doi.org/10.1016/j.cemconres.2025.107983.
[20] X. Liu, P. Wu, X. Liu, Z. Zhang, X. Ai, The utilization of carbonated steel slag as a supplementary cementitious material in cement, Materials 17 (18) (2024) 4574, https://doi.org/10.3390/ma17184574.
[21] X. Li, H. Mehdizadeh, T.C. Ling, Environmental, economic and engineering performances of aqueous carbonated steel slag powders as alternative material in cement pastes: Influence of particle size, Sci. Total. Environ. 903 (2023) 166210, https://doi.org/10.1016/j.scitotenv.2023.166210.
[22] G. Biava, M. Zajac, A. Principigallo, L.E. Depero, M.B. Haha, E. Bontempi, Evaluation of steel slags in CO_2 sequestration and as supplementary cementitious material, Constr. Build. Mater. 489 (2025) 142271, https://doi.org/10.1016/j.conbuildmat.2025.142271.
[23] T.C. Alex, G. Mucsi, T. Venugopalan, S. Kumar, BOF steel slag: critical assessment and integrated approach for utilization, J. Sustain. Metall. 7 (4) (2021) 1407–1424, https://doi.org/10.1007/s40831-021-00435-2.
[24] P. Liu, L. Mo, Z. Zhang, Effects of carbonation degree on the hydration reactivity of steel slag in cement-based materials, Constr. Build. Mater. 370 (2023) 130653, https://doi.org/10.1016/j.conbuildmat.2023.130653.
[25] P. Thongsanitgarn, W. Wongkeo, A. Chaipanich, C.S. Poon, Heat of hydration of Portland high-calcium fly ash cement incorporating limestone powder: Effect of limestone particle size, Constr. Build. Mater. 66 (2014) 410–417, https://doi.org/10.1016/j.conbuildmat.2014.05.060.
[26] Y. Li, H. Mehdizadeh, K.H. Mo, T.C. Ling, Co-utilization of aqueous carbonated basic oxygen furnace slag (BOFS) and carbonated filtrate in cement pastes considering reaction duration effect, Cem. Concr. Compos. 138 (2023) 104988, https://doi.org/10.1016/j.cemconcomp.2023.104988.
[27] S. Srivastava, M. Cerutti, H. Nguyen, V. Carvelli, P. Kinnunen, M. Illikainen, Carbonated steel slags as supplementary cementitious materials: reaction kinetics and phase evolution, Cem. Concr. Compos. 142 (2023) 105213, https://doi.org/10.1016/j.cemconcomp.2023.105213.
[28] H. Wang, Z. Ma, L. Jiang, L. Peng, G. Xiong, Y. Jiang, C.S. Poon, Enhanced reactivity of basic oxygen furnace slag by modified carbonation: comparison among different calcium carbonate polymorphs, Cem. Concr. Compos. 166 (2026) 106389, https://doi.org/10.1016/j.cemconcomp.2025.106389.
[29] Y. Tang, K. Schollbach, Z. Liu, S. van der Laan, W. Chen, H.J.H. Brouwers, Phosphate-activated basic oxygen furnace (BOF) slag: understanding pH-driven hydration and strength development, Cem. Concr. Res. 199 (2026) 108034, https://doi.org/10.1016/j.cemconres.2025.108034.
[30] B. Huo, B. Li, S. Huang, C. Chen, Y. Zhang, N. Banthia, Hydration and soundness properties of phosphoric acid modified steel slag powder, Constr. Build. Mater. 254 (2020) 119319, https://doi.org/10.1016/j.conbuildmat.2020.119319.
[31] B. Huo, B. Li, C. Chen, Y. Zhang, Surface etching and early age hydration mechanisms of steel slag powder with formic acid, Constr. Build. Mater. 280 (2021) 122500, https://doi.org/10.1016/j.conbuildmat.2021.122500.
[32] B. Huo, B. Li, C. Chen, Y. Zhang, D. Wang, Morphological and mineralogical insights into acetic acid modifying and hydraulic process on steel slag for enhanced reactivity, Constr. Build. Mater. 307 (2021) 125004, https://doi.org/10.1016/j.conbuildmat.2021.125004.
[33] R. Ragipani, S. Bhattacharya, A.K. Suresh, A review on steel slag valorisation via mineral carbonation, React. Chem. Eng. 6 (7) (2021) 1152–1178, https://doi.org/10.1039/D1RE00035G.
[34] K. Cao, L. Wang, Y. Xu, W. Shen, H. Wang, The hydration and compressive strength of cement mortar prepared by calcium acetate solution, Adv. Civil. Eng. 2021 (1) (2021) 8817725, https://doi.org/10.1155/2021/8817725.
[35] D.D. Nguyen, P.T. Quynh, Effect of calcium acetate on some properties of blended portland cement, J. Mater. Constr. 15 (01) (2025) 180, https://doi.org/10.54772/jomc.v15i01.1010.
[36] K. Binnemans, P.T. Jones, Á. Manjón Fernández, V. Masaguer Torres, Hydrometallurgical processes for the recovery of metals from steel industry by-products: a critical review, J. Sustain. Metall. 6 (4) (2020) 505–540, https://doi.org/10.1007/s40831-020-00306-2.
[37] S.Y. Pan, R. Adhikari, Y.H. Chen, P. Li, P.C. Chiang, Integrated and innovative steel slag utilization for iron reclamation, green material production and CO_2 fixation via accelerated carbonation, J. Clean. Prod. 137 (2016) 617–631, https://doi.org/10.1016/j.jclepro.2016.07.112.
[38] A.S. Reddy, R.K. Pradhan, S. Chandra, Utilization of basic oxygen furnace (BOF) slag in the production of a hydraulic cement binder, Int. J. Mineral. Process. 79 (2) (2006) 98–105, https://doi.org/10.1016/j.minpro.2006.01.001.
[39] K. Song, S. Park, W. Kim, C.W. Jeon, J.W. Ahn, Effects of experimental parameters on the extraction of silica and carbonation of blast furnace slag at atmospheric pressure in low-concentration acetic acid, Metals 7 (6) (2017) 199, https://doi.org/10.3390/met7060199.
[40] X. Mei, Q. Zhao, Y. Min, C. Liu, P. Shi, H. Saxén, R. Zevenhoven, Dissolution behavior of steelmaking slag for Ca extraction toward CO_2 sequestration, J. Environ. Chem. Eng. 11 (3) (2023) 110043, https://doi.org/10.1016/j.jece.2023.110043.
[41] J.L. Klug, S.L. Medeiros, H. Caldas, M. Bentes, H. Becker, Separation of iron and calcium from a BSSF steelmaking slag through acid leaching, Mater. Res. 25 (2022) e20210571, https://doi.org/10.1590/1980-5373-mr-2021-0571.
[42] L. Liu, X. Fan, M. Gan, J. Wei, Z. Gao, Z. Sun, J. Li, Microwave-enhanced selective leaching calcium from steelmaking slag to fix CO_2 and produce high value-added CaCO3, Sep. Purif. Technol. 330 (2024) 125395, https://doi.org/10.1016/j.seppur.2023.125395.
[43] G. Ferrara, P. Humbert, D. Garufi, P. Palmero, Evolution of CO_2 uptake degree of ordinary Portland cement during accelerated aqueous mineralisation, Ceramics 7 (4) (2024) 1711–1726, https://doi.org/10.3390/ceramics7040109.
[44] T. Matschei, S. Braymand, N. Garg, B. Huet, D. Jansen, R.J. Myers, P. Suraneni, Test methods for CO_2 mineralization in cement-based materials: a review by RILEM TC 309-MCP, Mater. Struct. 59(4) 175 (2026), https://doi.org/10.1617/s11527-026-03064-x.

[45] S. Seesanong, C. Seangarun, B. Boonchom, N. Laohavisuti, W. Boonmee, S. Thompho, P. Rungrojchaipon, Low-cost and eco-friendly calcium oxide prepared via thermal decompositions of calcium carbonate and calcium acetate precursors derived from waste oyster shells, Materials 17 (15) (2024) 3875, https://doi.org/10.3390/ma17153875.
[46] ASTM C1897–20 - Standard Test Methods for Measuring the Reactivity of Supplementary Cementitious Materials by Isothermal Calorimetry and Bound Water Measurements (2020).
[47] J. Hu, Z. Ge, K. Wang, Influence of cement fineness and water-to-cement ratio on mortar early-age heat of hydration and set times, Constr. Build. Mater. 50 (2014) 657–663, https://doi.org/10.1016/j.conbuildmat.2013.10.011.
[48] X. Li, R. Snellings, M. Antoni, N.M. Alderete, M. Ben Haha, S. Bishnoi, K. L. Scrivener, Reactivity tests for supplementary cementitious materials: RILEM TC 267-TRM phase 1, Mater. Struct. 51(6) 151 (2018), https://doi.org/10.1617/s11527-018-1269-x.
[49] BS EN, 196–1 - Methods of testing cement: Determination of strength, British Standards Institution (2016).
[50] EN 1015–3, Methods of Test Mortar for Masonry. Determination of Consistence of Fresh Mortar (By Flow Table), (1999).
[51] K. Zhang, Q. Cang, L. Peng, Y. Wang, S. Zhang, H. Li, Y. Wang, The mechanism of calcium leaching from steel slag based on the “water-acetic acid” two-step leaching route, Processes 13 (12) (2025) 4077, https://doi.org/10.3390/pr13124077.
[52] G. Chen, S. Bian, J. Gao, P. Jin, R. Wang, Effect and mechanism of acetic acid to improve the hydration activity of steel slag, Jom 75 (4) (2023) 1079–1088, https://doi.org/10.1007/s11837-022-05574-9.
[53] K. Luo, W. Zhang, J. Ye, J. Li, Z. Lu, X. Ren, Mechanism of interaction between hydration–carbonation of C2S, Constr. Build. Mater. 412 (2024) 134891, https://doi.org/10.1016/j.conbuildmat.2024.134891.
[54] Ç.M. Oral, B. Ercan, Influence of pH on morphology, size and polymorph of room temperature synthesized calcium carbonate particles, Powder Technol. 339 (2018) 781–788, https://doi.org/10.1016/j.powtec.2018.08.066.
[55] F. Zunino, K. Scrivener, The influence of the filler effect on the sulfate requirement of blended cements, Cem. Concr. Res. 126 (2019) 105918, https://doi.org/10.1016/j.cemconres.2019.105918.
[56] L. Chen, H. Wang, K. Zheng, J. Zhou, F. He, Q. Yuan, The mechanism of basic oxygen furnace steel slag retarding early-age hydration of Portland cement and mitigating approach towards higher utilization rate, J. Clean. Prod. 362 (2022) 132493, https://doi.org/10.1016/j.jclepro.2022.132493.
[57] A. Jexembayeva, T. Salem, P. Jiao, B. Hou, R. Niyazbekova, Blended cement mixed with basic oxygen steelmaking slag (BOF) as an alternative green building material, Materials 13 (14) (2020) 3062, https://doi.org/10.3390/ma13143062.
[58] L. Li, X. Wu, C. Wang, T.C. Ling, Carbonated steel slag as supplementary cementitious material: paving the way to full reutilization, Case Stud. Constr. Mater. 22 (2025) e04535, https://doi.org/10.1016/j.cscm.2025.e04535.